NAVAL POSTGRADUATE SCHOOL
Monterey, California

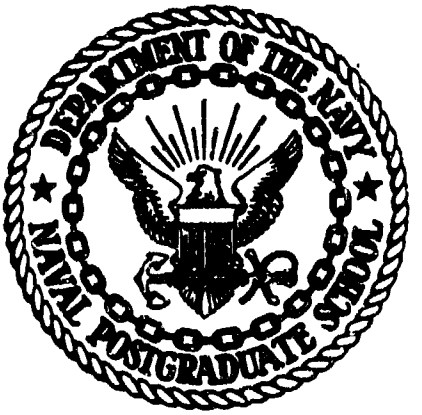

THESIS

AN INVESTIGATION OF THE HOT CORROSION PROTECTIVITY BEHAVIOR OF PLATINUM MODIFIED ALUMINIDE COATINGS ON NICKEL-BASED SUPERALLOYS

by

Rudolph E. Malush

March 1987

Thesis Advisor: D.H. Boone

SECURITY CLASSIFICATION OF THIS PAGE

REPORT DOCUMENTATION PAGE

1a REPORT SECURITY CLASSIFICATION: UNCLASSIFIED	1b RESTRICTIVE MARKINGS
2a SECURITY CLASSIFICATION AUTHORITY	3 DISTRIBUTION/AVAILABILITY OF REPORT: Approved for public release; distribution is unlimited.
2b DECLASSIFICATION/DOWNGRADING SCHEDULE	
4 PERFORMING ORGANIZATION REPORT NUMBER(S)	5 MONITORING ORGANIZATION REPORT NUMBER(S)
6a NAME OF PERFORMING ORGANIZATION: Naval Postgraduate School; 6b OFFICE SYMBOL (If applicable): 69	7a NAME OF MONITORING ORGANIZATION: Naval Postgraduate School
6c ADDRESS (City, State, and ZIP Code): Monterey, California 93943-5000	7b ADDRESS (City, State, and ZIP Code): Monterey, California 93943-5000
8a NAME OF FUNDING/SPONSORING ORGANIZATION; 8b OFFICE SYMBOL (If applicable)	9 PROCUREMENT INSTRUMENT IDENTIFICATION NUMBER
8c ADDRESS (City, State, and ZIP Code)	10 SOURCE OF FUNDING NUMBERS: PROGRAM ELEMENT NO; PROJECT NO; TASK NO; WORK UNIT ACCESSION NO

11 TITLE (Include Security Classification)
AN INVESTIGATION OF THE HOT CORROSION PROTECTIVITY BEHAVIOR OF PLATINUM MODIFIED ALUMINIDE COATINGS ON NICKEL-BASED SUPERALLOYS

12 PERSONAL AUTHOR(S)
Malush, Rudolph E.

13a TYPE OF REPORT	13b TIME COVERED FROM ____ TO ____	14 DATE OF REPORT (Year, Month, Day)	15 PAGE COUNT
Master's Thesis		1987 March	101

16 SUPPLEMENTARY NOTATION

17 COSATI CODES		
FIELD	GROUP	SUB-GROUP

18 SUBJECT TERMS (Continue on reverse if necessary and identify by block number)
Turbines, Blades, Coatings, Platinum Aluminides, Chromium Aluminides, Hot Corrosion

19 ABSTRACT (Continue on reverse if necessary and identify by block number)

The adverse operating environments encountered by marine gas turbine components has necessitated the development of various protective coating systems. Diffusion aluminide coatings have been used successfully for many years to enhance the hot corrosion resistance of turbine blades and vanes. Recently, it has been found that by modifying these standard aluminide coatings with a thin platinum underlay, significant improvements in high temperature corrosion resistance can be achieved. Using a laboratory furnace specifically modified to reproduce hot corrosion attack morphologies, the effects of selected platinum-aluminide

20 DISTRIBUTION/AVAILABILITY OF ABSTRACT	21 ABSTRACT SECURITY CLASSIFICATION	
☒ UNCLASSIFIED/UNLIMITED ☐ SAME AS RPT ☐ DTIC USERS	UNCLASSIFIED	
22a NAME OF RESPONSIBLE INDIVIDUAL: D. H. Boone	22b TELEPHONE (Include Area Code): (415) 938-4780	22c OFFICE SYMBOL: 69Bl

DD FORM 1473, 84 MAR — 83 APR edition may be used until exhausted; All other editions are obsolete — SECURITY CLASSIFICATION OF THIS PAGE

(19. continued)

cont'd → coating deposition variables were investigated on two nickel-base superalloy substrates (~~IN-100 and IN-738~~).

(Keywords:

Approved for public release; distribution is unlimited

An Investigation of the Hot Corrosion Protectivity Behavior of Platinum Modified Aluminide Coatings on Nickel-Based Superalloys

by

Rudolph E. Malush
Lieutenant, United States Navy
B.S., Pennsylvania State University, 1978

Submitted in partial fulfillment of the requirements for the degrees of

MASTER OF SCIENCE IN MECHANICAL ENGINEERING
and
MECHANICAL ENGINEER

from the

NAVAL POSTGRADUATE SCHOOL

March 1987

Author: Rudolph E. Malush
Rudolph E. Malush

Approved by: D.H. Boone, Thesis Advisor

T.R. McNelley, Second Reader

A.J. Healey, Chairman,
Department of Mechanical Engineering

G.E. Schacher
Dean of Science and Engineering

ABSTRACT

The adverse operating environments encountered by marine gas turbine components has necessitated the development of various protective coating systems. Diffusion aluminide coatings have been used successfully for many years to enhance the hot corrosion resistance of turbine blades and vanes. Recently, it has been found that by modifying these standard aluminide coatings with a thin platinum underlay, significant improvements in high temperature corrosion resistance can be achieved. Using a laboratory furnace specifically modified to reproduce hot corrosion attack morphologies, the effects of selected platinum-aluminide coating deposition variables were investigated on two nickel-base superalloy substrates (IN-100 and IN-738).

TABLE OF CONTENTS

ACKNOWLEDGEMENTS

I would like to take this opportunity to thank the many people who contributed to the completion of this thesis. The advice and patience of Dr. D.H. Boone and the generous technical support of Mr. Colin Thomas of Howmet Corporation, Dr. S. Shankar of Turbine Components Corporation, and Mr. Tony Gallinoto of EMTEK Applied Research Labs are gratefully acknowledged. I would also like to express my sincere appreciation for the technical guidance and assistance provided by Dr. Prabir Deb and Mrs. Tammy Bloomer which were instrumental to the completion of this research. Special thanks goes to Ms. Drue Porter whose concentrated clerical/organizational efforts provided an invaluable service at a time when it was most needed. Last, but certainly not least, I wish to thank my wife, Suzanne, and son Ethan for patiently following this investigation to its completion and persevering through "one last deployment". To the two of you, I dedicate all I have done.

I. INTRODUCTION

The United States Navy is presently engaged in some of the most ambitious ship acquisition programs instituted since the end of World War II. Virtually all new combatants entering the fleet or currently under construction will rely on the marine gas turbine, not only for their main propulsion requirements, but ships service power generation as well. Some inherent advantages afforded by gas turbines include compact installation, rapid startups from cold iron, quick power response, as well as reduced maintenance downtime associated with its modular construction. Due mainly to these assets, the propulsor selected for use aboard the DD-963 SPRUANCE class destroyers, FFG-7 PERRY class frigates, and CG-47 TICONDEROGA class cruisers was the LM2500 gas turbine engine. [Ref. 1]

The LM2500 is a marinized derivative of the CF6/TF39 aircraft engine core which had proven to be a reliable prime mover for the C5A transport aircraft. In order to evaluate the in-service performance and environmental resistance of LM2500 components, the MSC container ship CALLAGHAN was converted for use as a marine gas turbine test platform. During the initial performance trials conducted in the late 1960's, it was assumed that sustained, full power test runs would provide the most adverse engine operating environment

possible. This assumption had been based on previous aircraft engine corrosion experience which had shown that high temperature hot corrosion of the first stage HP turbine blades was normally a major life-limiting consideration. However, as the LM2500 test program continued, it was unexpectedly discovered that at low engine power levels, corrosion rates were actually much greater than those previously experienced during high power operation. These findings were substantiated by similar observations made by NAVAIR involving low-flying aircraft that operated in close proximity to marine environments. This was the Navy's first encounter with the marine-induced degradation mechanism most commonly referred to as low temperature hot corrosion. [Ref. 2]

By the early 1970's, several NAVSEA sponsored research efforts were underway in an attempt to characterize this previously unrecognized form of hot corrosion and to determine the kinetics involved. Concurrently, in an attempt to improve turbine blade life, multistage filtration demisters were installed in the ship's air intake plenums to prevent the ingestion of sea salts directly into the engine. It was quickly realized, however, that even the most elaborate air filtration schemes were still only partially successful in extracting seawater aerosols from the entering combustion air. Design and cost limitations dictated that other approaches be explored. Subsequent research revealed

that a reduction in the sulfur content of the fuel would also help reduce the rate of hot corrosion attack. The additional distillation processing that would be required, however, was found to be both involved and uneconomical. These processing difficulties made it strategically impractical to commit naval ships to higher grades of fuel which might not be as readily available. [Ref. 3]

The final option available to design engineers was to improve the hot corrosion resistance of the turbine blade materials themselves. The approach that had been taken in blade development to date was to utilize nickel and cobalt-based superalloys to provide the requisite high temperature strength and ductility while using diffusion aluminide coatings to furnish the necessary surface stability and high temperature corrosion resistance. However, since the service life of marine gas turbines was still significantly shorter than their aircraft engine counterparts, expanded basic research in superalloy development and coating system design became a high priority item. As a result of this research it was determined that diffusion aluminide coatings modified by an initial platinum underlay significantly improved the overall hot corrosion resistance, especially in the high temperature regime (800-1000°C). These coating types with their improved protectivity characteristics have been the major thrust of an ongoing research effort here at the Naval Postgraduate School. This NAVAIR sponsored study

is an extension of that previous research and attempts to further clarify substrate/coating interactions and the structural effects that may be involved, while screening new platinum-aluminide coating systems in order to rank their relative hot corrosion resistance capabilities.

II. BACKGROUND

A. SUPERALLOY MATERIALS

Historically, the evolution of the gas turbine engine design has been substantially controlled by advances made concurrently in the field of high temperature materials. Since its inception, the major limitation to improved engine performance has invariably been connected to the maximum allowable temperature within the high pressure turbine inlet immediately following the combustor. Ideally, only high strength, temperature-capable alloys with inherently high environmental resistance should be utilized in these critical engine areas. Unfortunately, alloy compositions chosen to optimize the thermo-mechanical criteria for gas turbine applications are generally less capable in the area of hot corrosion resistance and a performance compromise has had to be made. The current materials approach has been to develop turbine component base metals which provide not only the requisite high temperature mechanical properties, but a moderate environmental resistance as well. Additional surface stability is then furnished through the application of a corrosion resistance coating to the airfoil hot-gas-path surfaces. The enhanced protectivity afforded by this coating is derived from its ability to form a stable surface

oxide layer without significantly degrading the mechanical properties of the underlying substrate metal.

Superalloys, the materials employed within marine gas turbines, must possess a broad spectrum of thermal and mechanical properties. These complex alloy systems generally consist of nickel or cobalt as their principal constituent with small to moderate percentages of up to twelve alloying elements added to achieve the desired material characteristics. The properties generally considered most essential for gas turbine applications include:

1. an ability to maintain creep-rupture strength at elevated temperatures
2. sufficient ductility throughout a broad temperature range to resist brittle fracture
3. light weight but with a high stiffness coefficient
4. good thermal fatigue resistance
5. some inherent resistance to surface degradation by oxidation and hot corrosion.

The choice of which superalloy to use for a particular engine component is usually dictated by the anticipated temperature/stress conditions and specific duty cycle involved. Cobalt-based superalloys are intrinsically more temperature-capable and corrosion resistant than their nickel-based counterparts, due in part to their high cobalt and chromium contents respectively. Their load bearing capabilities are somewhat limited, however, and are therefore used primarily for combustor sheeting and nozzle guide

vanes. Nickel-based superalloys, on the other hand, generally have a lower melting temperature yet much greater residual creep strength and are used mainly for turbine blading as well as some of the later stage vanes.

Nickel-based superalloys derive their high strength from a fine assemblage of ordered gamma prime (γ') cuboids embedded in a disordered gamma (γ) phase matrix. The γ' phase refers to any of the ordered second phase intermetallic compounds formed from nickel and either aluminum, titanium, niobium, or tantalum (or combination thereof). The coherent face-centered cubic stucture of the γ' crystals is highly resistant to deformation, particularly at elevated temperatures, which enables it to effectively pin moving dislocations in place. The resultant coherency strains make it much more difficult for single dislocations to transit through the microstructure thereby strengthening the superalloy considerably. In general, the more γ' phase precipitates present, while still maintaining a continuous γ phase matrix, the stronger the material becomes. [Ref.4]

In nickel-based superalloys, additional mechanical strength can be achieved by adding small amounts of molybdenum or tungsten to form second phase carbides which contribute to grain boundary strengthening. Additions of cobalt will raise the γ' solvus temperature, thus enhancing high temperature capabilities, while aluminum and chromium both form protective oxides which improve hot corrosion

resistance. Unfortunately, the same increases in chromium which are used to improve environmental resistance, decrease the γ' solvus temperature and therefore degrade the alloy's maximum useful strength. With technological pressure for improved creep strength at increasingly higher operating temperatures, there has been a tendency to increase the amount of the γ' forming elements at the expense of the overall chromium content. This concomitant reduction in chromium has in turn substantially reduced the intrinsic hot corrosion resistance of nickel-based superalloys. This dilemma led to a reassessment of turbine blade design criteria and necessitated increases in material complexity through the use of protective coating systems. Today, virtually all marine gas turbine hot-gas-path components are protected with coatings. [Ref. 5]

B. CORROSION MECHANISMS

The surface degradation of marine gas turbine components is mainly the result of three distinctly separate modes of attack. These known mechanisms for which specific morphologies have been identified include high temperature oxidation, low temperature hot corrosion (LTHC), and high temperature hot corrosion (HTHC). At temperatures below 600°C corrosion attack is relatively insignificant since contaminants are in the solid phase with little propensity to form molten deposits on airfoil surfaces. Above 800°C high temperature oxidation begins to become significant, and

at temperatures in excess of 1000°C it emerges as the dominant mode of surface attack. In the intervening temperature region, two morphologically unique forms of accelerated corrosion occur. These two modes are collectively referred to as hot corrosion, which has been further subdivided into the low temperature (600-800°C) regime and the high temperature (800-1000°C) regime. All three of these temperature dependent mechanisms are particularly aggressive in the marine environment and can quickly become performance limiting, especially for those engine components having close life-time tolerances by design. [Ref. 6]

1. High Temperature Oxidation

Oxidation of superalloy components occurs when hot combustion gases, which invariably contain a residual partial pressure of oxygen, come in contact with exposed metal atoms to form metallic oxide(s). These surface oxides have a lower overall activity than the base metal from which they were produced. Susceptibility of a particular metal surface to oxidation is therefore dependent upon the free energy of formation of its metallic oxide. This Gibbs free energy is reduced (facilitating oxidation) by increased temperatures and oxygen partial pressures. Surface oxidation of a metal is particularly difficult to suppress at high temperatures since oxide formation is thermodynamically favorable for most metals even in the presence of extremely small amounts of oxygen. Since new oxide scale formation is

restricted to the scale/metal interface, oxygen ions must diffuse in through the scale layer or metal ions must diffuse outward to sustain the reaction. This initial oxide layer can therefore serve as a diffusion barrier preventing further attack of the underlying metal, provided it has a relatively low diffusivity for O_2 or metal ions, can resist cracking, and remains adherent. [Refs. 7,8]

In most contemporary superalloy systems, oxidation rates can be reduced through the formation of a selected oxide layer. What this process entails is for one of the alloying elements to be selectively oxidized to form its metal oxide, thereby suppressing the oxide formation of the other elements which have less affinity for the oxygen. In the initial stages of high temperature oxidation, exposed metal atoms on the surface compete in oxide formation until the most thermodynamically stable oxide dominates. As a result of its formation kinetics, which favor lateral growth, this dominant protective oxide continues to grow until it forms a continuous surface layer. At this point, there is a parabolic decrease in the rate of oxidation and the surface stabilizes. If, on the other hand, the dominant oxide that forms turns out to be porous, discontinuous, or non-adherent, metal oxidation rates will not slow and component failure will become an eventuality. [Ref. 9]

Nickel-based superalloys principally develop a selective oxide layer of chromia (Cr_2O_3), although the

preferred alumina (Al_2O_3) can also be formed. High temperature cyclic exposure and oxide growth stresses have a tendency to crack these protective scales, which can then spall off leaving behind localized patches of unoxidized metal. Protective surface oxides will continue to reform by a selected oxidation of the chromium (or aluminum) until these elements reach a critical level of depletion locally within the substrate. At this point, less stable oxides such as NiO or CrO begin to dominate, accompanied by an accelerated rate of oxidation attack. [Refs. 9,10]

2. High Temperature Hot Corrosion

High temperature hot corrosion (HTHC) is an aggressive, accelerated form of oxidation which attacks marine gas turbine blades and vanes directly exposed to the flow of hot combustion gas products. HTHC occurs primarily as a result of sodium salts which enter with the intake air, reacting with contaminants ingested with the fuel to form sodium sulfate (Na_2SO_4) and related compounds such as V_2O_5. Sodium sulfate along with the vanadates (V_2O_5, etc.) can then form molten deposits on the surface of gas turbine airfoils. This molten salt mixture in the presence of a partial pressure of SO_2/SO_3 provided by the combustion gases, generates a fluxing (dissolving) of the protective oxide scale and inhibits its reformation. If allowed to progress unchecked, catastrophic attack of the underlying substrate metal will result. [Ref. 11]

HTHC is often referred to as Type I hot corrosion since it was the first unique morphology encountered. HTHC is most prevalent in the 800-1000°C temperature range and is easily recognized by a characteristic zone of aluminum depletion in advance of the corrosion front. A second common feature of HTHC attack is the presence of sulfide phase (AlS, CrS) byproducts contained within the aluminum depletion zone. These sulfides may form along grain boundaries or exist as independent extrusions which impart a rough, mottled appearance to this type of attack. Interestingly, it was due to these sulfides that the misnomer "sulfidation" attached itself to HTHC. [Ref. 12]

The kinetics of HTHC can be viewed as a two stage process of initiation and propagation. The first stage, initiation, does not require the presence of a contaminating mixture of sulfates and (SO_2/SO_3) generally associated with hot corrosion. During this stage, the degradation process is relatively slow, as an initial reaction product scale forms in a manner similar to simple oxidation. Chromium and aluminum diffuse outward to form an internal oxide layer underneath the external surface scale. This internal oxide layer forms a protective barrier which continues to be replenished as required by the diffusion of chromium and aluminum from the surrounding substrate. The initiation stage ends when this local chromium/aluminum reservoir

becomes sufficiently depleted to allow the surface barrier to be effectively penetrated. [Ref. 11]

The second stage, propagation, proceeds at a much faster rate than initiation. The salt fluxing reactions that occur in this stage can be viewed as either basic or acidic. Basic fluxing occurs when there is a reaction between oxide ions generated by sodium sulfate dissociation within the deposit and the outer protective oxide scale. For basic fluxing to sustain its corrosive attack, the sodium sulfate must be continually renewed. On the other hand, acidic fluxing, which is considered to be much more devastating, involves the transport of oxide ions from the protective oxide scale to the molten deposit. Acidic fluxing reactions can be further subdivided into alloy induced or gas phase induced, depending on the source of the acidic component. Alloy induced acidic fluxing occurs when the superalloy refractory metals (i.e., molybdenum, tungsten, and vanadium) form oxides in the sodium sulfate deposit. These refractory metal oxides cause the deposit to become acidic which permits this particular HTHC mechanism to become self-sustaining without the necessity for additional sodium sulfate. Conversely, gas phase induced acidic fluxing occurs when the presence of an acidic component of the combustion gas products (SO_3) generates a deficiency of oxide ions within the sodium sulfate deposit. The protective oxide layer then dissociates as it furnishes oxide ions

to the deposit. A continual supply of sulfur trioxide would therefore be required to sustain this gas phase induced fluxing reaction. [Ref. 11]

Any number of these mechanisms may be present under specific operating conditions, however, sulfur induced degradation, basic fluxing, and alloy induced acidic fluxing are normally the only ones of significance in the HTHC temperature regime. Gas phase induced acidic fluxing is generally associated with corrosion at lower temperatures (650-750°C) and is considered to be the principle mechanism for LTHC. Table I includes an overall summary of the hot corrosion mechanisms and their most probable formation reactions. [Refs. 11,13]

3. Low Temperature Hot Corrosion

As demonstrated aboard the GTS CALLAGHAN, marine gas turbine engines operating at reduced power levels experienced a more devastating corrosion attack than those previously tested at high power. This new form of degradation was designated Type II hot corrosion and was found to occur in the 600-800°C temperature range, well below the Na_2SO_4 melting point of 884°C. This inconsistency can be accounted for by the fact that a molten eutectic combination such as (Na_2SO_4 + $NiSO_4$), with a melting point as low as 575°C, actually condenses onto the airfoil surfaces at these lower temperatures. This molten salt mixture penetrates into the oxide layer at cracks and other surface

imperfections resulting in severe localized pitting as shown in Figures B.13(a) and B.15(a). In addition to this characteristic pitting, there is also a sharply defined corrosion front with few sulfides and no aluminum depletion zone associated with this form of attack. [Ref. 11]

The preferential removal of aluminum from the superalloy surface during LTHC again occurs as a two stage process. The first stage, initiation, can be regarded as the formation of a molten eutectic salt deposit on the engine component surface. LTHC then propagates by a gas phase induced acidic fluxing which requires a constant supply of sulfite (SO_3) at the liquid/alloy interface and the presence of O_2 and SO_2 partial pressure gradients across the deposit. At these lower temperatures, the presence of the SO_3 further suppresses the melting point of sodium sulfate and results in an accelerated sulfur transfer through the melt. Aluminum and sulfite ions then react to form $Al_2(SO_3)_3$ which is stable due to the existence of a high SO_3/O_2 partial pressure ratio at the salt/alloy interface. As the $Al_2(SO_3)_3$ diffuses away from this interface to areas of the melt where the partial pressure of O_2 is higher, a free energy reduction again favors the formation of the metal oxide phase resulting in a reprecipitation of Al_2O_3. This relocated Al_2O_3 is no longer part of the continuous surface oxide layer, but rather a dispersion of non-protective precipitates. [Ref. 11]

As temperatures increase, the SO_3 pressure decreases, so there is less likelihood of forming the conditions necessary to initiate acidic fluxing reactions. This situation arises since the sulfide ions form a larger proportion of the SO_2/SO_3 equilibrium combination at these higher temperatures. Therefore, the extensive surface pitting generated during the LTHC process normally diminishes above 800°C where then HTHC becomes the more dominant mode of attack. Figure B.1 displays the relative rates at which these two general forms of hot corrosion occur and the temperature ranges where they become most dominant.[Ref. 11]

C. PROTECTIVE COATING SYSTEMS

The wide variety of hot corrosion mechanisms and the broad temperature ranges in which they occur, presents a multifaceted challenge to the developers of superalloy protective coatings. These coating systems must depend upon the stability and effectiveness of metal oxide reaction products to form an environmental barrier against further oxidation and hot corrosion attack. In addition to enhancing surface capabilities, the following basic coating system design requirements must be considered:

1. High mechanical strength is necessary, but with sufficient inherent ductility to accommodate substrate dimensional changes during transient loading conditions.

2. Chemical compatibility with the superalloy substrate must exist so that the coating will remain adherent. Heat treating the applied coating can promote better adherence, however, pronounced interdiffusion of coating elements with the substrate can degrade both the coating's ability to maintain a continuous protective barrier and substrate mechanical properties through dilution effects. Additionally, improper diffusion heat treatments can result in a growth or resolution of superalloy strengthening phases further reducing the component's mechanical integrity.
3. Compatibility between coating and substrate thermal expansion coefficients must exist to prevent mismatch induced strains and thermal fatigue cracking from occurring during service.
4. Total cost of the coating in relation to the component's equivalent service life extension must be considered. This cost analysis should include some input as to the coating's ability to be reconditioned and the complexity of the processes required.
5. Careful quality control must exist during the coating deposition process to prevent blocking or otherwise constricting any of the elaborate internal cooling passages that commonly exist within advanced gas turbine components. Blade dimensional tolerances must be closely monitored to prevent excessive coating

buildups from interfering with the aerodynamic efficiency of the engine. [Ref. 14]

The three most widely used high temperature coatings are the thermal barrier, the overlay or metallic cladding, and the diffusion type. Ceramic thermal overlays are applied to enhance the service life of low-load bearing engine components such as sheet metal combustion liners and exhaust ducts. This type of coating offers the dual advantage of excellent environmental resistance along with high insulative qualities which effectively lowers the substrate metal temperature. This permits higher turbine inlet temperatures to be utilized and also reduces cooling air requirements. Although attempts have been made to use thermal barrier coatings on more highly loaded turbine airfoils, limited success has been achieved due mainly to adherence problems and the inherently brittle nature of ceramics. [Ref. 15]

Overlay coatings are essentially metallic claddings, applied by a line-of-sight plasma spray or physical vapor deposition (PVD) technique. These metallic overlays are virtually independent systems as they do not significantly interact with the underlying substrate elements. Therefore, overlays degrade component mechanical properties to a much lesser extent than other coating types. This non-interactive feature allows the composition of overlays to be optimized to counterbalance anticipated environmental conditions. Difficulties have been encountered, however, in

the line-of-sight coating of internal cooling passages, deposition quality control, and in the containment of processing costs which combine to make this type of coating commercially less attractive. [Ref. 16]

Diffusion aluminide coatings are most commonly applied to superalloy components by an inexpensive method called pack cementation. This process is conducted in a retort containing a semi-permeable mixture of aluminum-rich metallic powders, a halide to achieve aluminum transport, and an inert diluent of refractory oxide powder. This pack mixture is then subjected to an appropriate heating schedule in order to produce a metallic halide vapor which effects the elemental transport of aluminum to the component surface. The resulting coating structure consists of an inner reaction-diffusion zone at the coating/substrate interface and one or two outer zones consisting of various aluminum-rich intermetallic compounds. These intermetallic compounds usually include a β (NiAl) phase for nickel-based superalloy substrates. Upon exposure to an oxidizing environment, a surface layer of alumina (Al_2O_3) forms which serves as an environmental barrier against further consumption of the base metal. If cyclic operating conditions should happen to crack or spall this protective oxide scale, the exposed unoxidized aluminide quickly reacts to form a new layer of protective alumina. This replenishment process will continue as long as a sufficient aluminum reservoir of

NiAl exists locally within the coating structure. Theoretically, this would imply that the thicker the applied coating, the more protection it would subsequently afford. Unfortunately, coatings thicker than about 75-100μm are not generally practical, as the high aluminum concentration will induce cracking. [Ref. 17]

By varying the aluminum activity in the pack and the deposition temperature, two archetypical coating structures will result. Diffusion coatings can be classified as either inward or outward, in reference to the initial method of aluminum incorporation in their formation.

1. Inward type coatings are formed by a low temperature high activity (LTHA) process which produces an inward diffusion of aluminum into the substrate during the aluminizing step. The high aluminum activity in the pack along with the relatively low processing temperature/time (760°C/1 hour) combine to generate a coating with a high aluminum gradient consisting mainly of an intermetallic phase based on δ (Ni_2Al_3). This as-formed coating of δ has a relatively low melting temperature and is much too brittle for practical use. The aluminizing treatment is therefore followed by a diffusion heat treatment (1080°C/4-6 hours) conducted within an inert environment to effect the transformation to and growth of a single β (NiAl) phase. This post-coating heat treatment also helps restore

substrate mechanical properties degraded during the aluminizing process. A three-zone coating structure consisting of an aluminum-rich β phase with substrate element precipitates typically emerges. The outer zone generally consists of a fine β phase with carbide precipitates distributed throughout. These substrate element carbides frequently extend out to the coating surface providing initiation sites that can accelerate local attack. The β phase intermediate zone is devoid of carbide precipitates and is often referred to as the "denuded zone". The inner coating layer is an interdiffusion zone composed primarily of a β (NiAl) matrix with an interdispersion of carbides and substrate element-rich precipitates. This zone is generally considered to be non-protective due to the presence of a brittle, finger-like σ (NiCr) phase which provides a ready avenue for the corrosion attack to reach the underlying substrate.

2. Outward type coatings are formed by a high temperature (1050°C/4 hours) low activity (HTLA) process. Due to this lower pack activity, aluminum is incorporated into the coating by way of an outward diffusion of nickel from the substrate through the β (NiAl) layer which produces a low gradient of aluminum. A two zone coating structure develops, with a nickel-rich outer layer of β devoid of precipitates from the original

substrate elements. Again, the interdiffusion zone is non-protective, comprised mainly of an aluminum-rich ß/nickle-poor substrate phase mixture. This zone also contains various precipitates formed from those elements of the alloy substrate not completely soluble within the ß. Since the HTLA process is conducted above the stability temperature of δ (Ni_2Al_3), subsequent heat treatments are not normally required. It should be noted, however, that HTLA coatings require significantly longer formation times than inward type coatings. This is a result, in part, of the low diffusion coefficient of nickel in ß forcing slower overall growth rates. Any foreign particles attached to the component surface prior to the aluminizing process will be entrapped within the interior of the coating, thereby marking the position of the initial surface. Metallic powders from the pack can become embedded in the external zone of the coating during the aluminizing step producing metallic inclusions which can modify the corrosion behavior of the coating considerably. Typical inward and outward aluminide coating structures are shown in Figures B.4(a) and B.6(a) respectively. [Ref. 18].

Many elements have been used in an attempt to modify conventional diffusion aluminide coatings. The most beneficial of these elements has been chromium and the noble

metals such as platinum. Normally a modified coating is formed through a two step deposition process. First a thin (6-12μm) layer of the modifying element (platinum) is electrodeposited onto the substrate surface and a diffusion heat treatment is performed to facilitate its bonding. For chromium modification, a vapor phase chromizing process is utilized. The modifying element is then incorporated into the coating during the subsequent aluminizing process (HTLA or LTHA). The structure of these modified coatings can be controlled by varying the modifying element deposition thickness, pre-aluminizing diffusion heat treatment parameters, and/or the aluminizing process itself to include its subsequent heat treatment schedule. [Ref. 19]

Chromium was one of the first elements used to modify aluminide coatings, and greatly enhanced LTHC resistance due to the formation of a protective layer of chromia (Cr_2O_3). This chromia layer, unfortunately, does not provide additional HTHC resistance as Cr_2O_3 volatilizes at temperatures above 850°C and prevents a continuous chromia layer from forming. Still chromium does contribute to HTHC resistance indirectly by decreasing the amount of aluminum required to form alumina (Al_2O_3) in nickel-aluminum systems. [Ref. 20]

The two general catagories of chromaluminide coatings which exist depend principally upon the method of aluminum incorporation used subsequent to the diffusion of chromium

into the substrate surface. These two archetype structures can be described as follows:

1. LTHA chromium-modified aluminides are formed by an inward diffusion of aluminum on a chromium enriched surface and exhibit a standard three zone structure.
    a. The outer zone consists of a NiAl matrix which is fully enriched with chromium (3 atom percent). Chromium in excess of this amount exists as a distribution of fine second phase α-Cr precipitates.
    b. The intermediate zone is a single phase β (NiAl) denuded of substrate element precipitates.
    c. The innermost layer is an interdiffusion zone consisting primarily of chromium carbides distributed in an NiAl matrix. [Ref. 21]
2. HTLA chromium-modified aluminides are developed by an outward diffusion of nickel and typically develop a two zone structure.
    a. The outer layer consists of a phase pure β (NiAl) matrix saturated with substrate elements that diffuse outward concurrently with the nickel. Due to the low solubility of chromium in NiAl, this zone has little chromium except for a lean distribution of pack mix particles embedded near the coating surface by the outward diffusion of nickel through the β.

b. The chromium enriched region between the phase pure NiAl outer layer and the interdiffusion zone serves as the inner zone. The chromium concentrates in this area to fill the void created by the outward diffusion of nickel. The inner zone contains a variety of refractory metal-rich precipitates such as chromium carbides, α-Cr, and TCP phases within an NiAl matrix. [Ref. 21]

More recently a layer of platinum has been electrodeposited onto the substrate surface prior to the aluminizing process on the premise that it would serve as a diffusion barrier permitting a greater proportion of the aluminum to remain near the coating surface. This concept was proven to be erroneous, however, as aluminum was found to freely diffuse through the platinum layer with the platinum remaining concentrated at the coating surface as $PtAl_2$ and Pt_2Al_3. Consequently, the platinum concentration gradient that develops is highest at the surface, but, rapidly diminishes as the interdiffusion zone is approached. [Ref. 22]

Platinum additions, nevertheless, greatly enhance the HTHC performance of diffusion aluminide coatings. Improvements of up to four times the oxidation resistance and six times the HTHC resistance have been reported. [Ref. 23]

These significant advances have been ascribed to the effect that platinum has on improving Al_2O_3 scale adhesion and cracking resistance, although the exact mechanisms have not been conclusively established as yet. Although platinum was found to significantly inhibit the basic fluxing mechanism of HTHC, it offered little improvement in suppressing the gas phase induced acidic fluxing of LTHC except when a "critical platinum-aluminum phase (possibly $PtAl_2$) is continuous at the coating surface". [Ref. 24] Attempts are currently underway to incorporate both chromium and platinum additions into commercial diffusion aluminide coatings in order to optimize their overall hot corrosion resistance capabilities. These triplex Pt-Cr-Al coatings develop some very complex structures and their formation mechanisms are still not well understood. [Ref. 25]

Boone and Deb [Refs. 26, 27, 28] have investigated the wide range of processing variables involved in forming platinum-aluminide coatings on IN-738 substrates and have characterized the resulting structures. Depending on the method of aluminum incorporation and the pre-aluminizing diffusion heat treatment used, four general categories of coatings structures result:

1. Inward type platinum-aluminide coatings are formed by employing a LTHA aluminizing process subsequent to the diffusion of a platinum layer into the substrate surface. By minimizing the pre-aluminizing diffusion

heat treatment, a single phase, four zone structure develops:

a. The surface zone consists of a platinum-rich single phase of $PtAl_2$. Random grit blast particles are generally present in a shallow zone at the initial substrate surface/platinum overlay interface. These particles serve as excellent diffusion markers indicating that the coating grows primarily by the inward diffusion of aluminum.

b. The outer intermediate zone is composed of either a fine assemblage of platinum-rich precipitates contained within an aluminum enriched NiAl matrix or aluminum-rich NiAl precipitate within a continuous $PtAl_2$ phase.

c. The inner intermediate zone is a single phase β (NiAl) rich in nickel and denuded or any other phases or substrate element precipitates.

d. The innermost zone is referred to as the interdiffusion zone and consists of an aluminum-rich β (NiAl) matrix with insoluble substrate elements and carbides distributed throughout.

Longer platinum pre-diffusion heat treatments result in a three zone coating structure as follows:

a. The outer zone consists of a platinum-rich $PtAl_2$ phase within an NiAl matrix rich in aluminum.

b. The intermediate zone is a single NiAl phase.

c. The innermost zone is again an interdiffusion zone as described above.

2. Outward type platinum-aluminide coating structures are formed using a HTLA aluminizing process resulting in a lower overall aluminum gradient. By minimizing the pre-aluminizing diffusion heat treatment, a two zone structure typically develops:

   a. The outer zone is a platinum-rich $PtAl_2$ phase.

   b. The intermediate zone consists of a $PtAl_2$ phase dispersed within a nickel-rich NiAl matrix.

   c. An interdiffusion zone is once again located between the intermediate zone and the underlying substrate.

Longer pre-diffusion heat treatments result in a two phase, three zone structure:

   a. The surface zone consists of a non-continuous layer of platinum-rich $PtAl_2$ precipitates contained within an aluminum-rich NiAl matrix.

   b. The intermediate zone is a single phase NiAl rich in nickel, void of any other phases or substrate element precipitates.

   c. The inner zone is the interdiffusion zone consisting primarily of refractory metal carbides in an NiAl matrix.

In all of the low activity Pt-Al coatings, stable substrate element carbides and pack grit particles (when present) are found throughout the inner coating zone. These particles serve as inert diffusion markers showing that the growth of the coating was predominantly by the outward diffusion of nickel.

Based upon the above background discussion of modified coating systems, it is readily apparent that a diversity of structures currently exist. By varying the sequence of the modifying element deposition and changing pre-aluminizing diffusion treatments/aluminizing processes, an attempt will be made to alter these standard structures in order to optimize their hot corrosion resistance capabilities.

III. EXPERIMENTAL PROCEDURES

A. BACKGROUND

In an attempt to simulate actual marine gas turbine service conditions in the laboratory, several accelerated hot corrosion test rigs have been devised. The more closely the experimental apparatus duplicates these dynamic hot corrosion conditions, the more complex, costly, and time consuming the testing becomes. Pressurized burner rigs and simple burner rigs are the two methods which strive to duplicate actual engine variables most realistically. Pressurized burner rigs simulate these conditions best by allowing complete control of the pressure, temperature, velocity and composition of the hot combustion gas products. Gas velocities as high as 2000 ft/sec have been attained, however, the production and operating costs of such complex test apparatus limits its utilization. Simple burner rigs, on the other hand, although unable to control the combustion gas pressure or velocity as closely, greatly reduce the overall expense and complexity of the requisite laboratory equipment. In both of these methods, higher than normal concentrations of seawater contaminants are injected into the combustion chamber air supply or dissolved into the fuel in an attempt to minimize the time required to produce measurable corrosion attack. [Ref. 29]

A third technique for conducting accelerated hot corrosion testing is through the use of a laboratory furnace. This method attempts to duplicate the actual local conditions which occur on the airfoil surfaces of a marine gas turbine engine (i.e., a salt deposit and a slight SO_2 + SO_3 overpressure). Test specimens are first sprayed with an aqueous salt solution, then dried and placed into the isothermal section of the furnace. An air/sulfur dioxide gas mixture flows through the furnace producing an aggressive environment in which hot corrosion readily occurs. The direct application of contaminating salt onto the specimens greatly accelerates the initiation stage of hot corrosion and produces significant coating degradation after only a few days of exposure. Because of its relative simplicity, this method is particularly useful in providing preliminary rankings of coating performance so that the most resistant coating systems can then be selected for further, more detailed evaluation.

B. EXPERIMENTAL APPARATUS

A horizontal, resistance-type l boratory furnace with a 2 1/2 inch ID Hastelloy-X furnace tube was specifically modified for use in hot corrosion studies at NPS. The furnace was calibrated such that a six inch isothermal hot zone existed in the center portion of the furnace. The hot zone temperature is able to be maintained to within ±5°C of

the desired set point temperature through the use of a proportional controller and digital pyrometer combination.

Low pressure compressed air is regulated and passed through moisture indicating "drierite" desiccant at a rate of 2000 ml/min. This dry air is mixed with anhydrous sulfur dioxide at a controlled flow rate of 5 ml/min to provide an overall 0.25 volume percent air/SO_2 mixture to the furnace front. The gas mixture enters the furnace and flows throughout its length contained within a 3/8 inch OD stainless steel tube in order to preheat the air/SO_2 mixture and obtain SO_2/SO_3 equilibrium prior to coming in contact with the test specimens. The spent gas mixture is exhausted through a flask of dilute sodium hydroxide solution to prevent any SO_2 from being discharged into the laboratory.

C. HOT CORROSION TESTING PROCEDURES

Commercially cast IN-100 and IN-738 pin-type specimens (approximately 0.6 centimeters in diameter) formed the basis for this investigation. The nominal weight percent compositions are delineated within Tables II and III. [Ref. 30] These cast superalloy pins were surface ground and solution heat treated prior to the commencement of the coating process. Platinum was initially electrodeposited onto the specimen surface to a thickness of 3-10 micrometers. This deposition was followed by a prealuminizing diffusion heat treatment conducted under vacuum. A specific aluminizing treatment (either HTLA or

LTHA) was then performed using a pack cementation or CVD process. A post coating heat treatment (1080°C/4 hours) normally followed to complete the coating process. The specimen coating descriptions, deposition variables, and other relevant parameters are summarized in Table IV.

The cylindrical-shaped pins received from the coating suppliers were sectioned into 2 centimeter test lengths suitable for use in the laboratory furnace. Additionally, a small sample was cut and mounted to provide "as received" coating microstructural baselines. Ends exposed by the cutting procedure were covered with an aluminum slurry repair compound to minimize the attack of these uncoated areas. (Additionally, no salt solution was applied to these endpieces.) Once dimensions were recorded, the surface area of each sample was calculated. The specimens were then cleaned with ethanol to remove surface oils and preheated in a convection oven at 170°C to evaporate any residual moisture. Using an analytical balance, the samples were weighed and then reheated in the convection oven for approximately twenty minutes to facilitate an even deposition of the contaminating salt. After removal from the oven a second time, and while still hot, salt in the form of a hydrated $Na_2SO_4/MgSO_4$ - 60/40 mole percent solution was sprayed onto the samples which were then inserted back into the oven to dry. The pin specimens were removed from the oven, cooled and reweighed on the

microbalance to determine the weight gain of salt that had been obtained. This procedure was repeated until a nominal salt weight gain equivalent to 1.5 mg/cm^2 was achieved for each specimen. For HTHC, where corrosion penetration rates are much lower, a nominal 2.0 mg/cm^2 coating was used to provide a more concentrated flux of molten salt.

After the salting procedure was completed, the specimens were placed in a specimen holder composed of Al_2O_3 base fire brick and inserted into the tube furnace hot zone. A hot zone temperature of 700°C was maintained during LTHC testing and 900°C for the HTHC runs. A flowing gas mixture consisting of 2000 ml/min of dry air and 5 ml/min of sulfur dioxide gas was established through the furnace rig. After a 20 hour exposure cycle in this corrosive environment, the specimens were removed from the furnace, air cooled to room temperature, visually examined, resalted and inserted back into the furnace for the next 20 hour cycle. For LTHC testing, a total of five 20 hour cycles produced an appropriate depth of corrosion attack, while for HTHC testing, ten 20 hour cycles of exposure were necessary. Specimen positions within the holder were rotated after each 20 hour cycle to ensure that any small temperature non-uniformities that existed within the furnace hot zone would have a minimal effect on the testing.

D. SPECIMEN PREPARATION AND DATA ACQUISITION

Upon completion of the requisite number of 20 hour cycles, both corroded and "as received" specimens were sectioned, mounted, and prepared for microscopic examination using standard metallographic procedures. A dilute HNO_3 based etchant (AG-21) was applied to the polished specimen surface to assist in developing contrast within the coating structure. A Zeiss light microscope with attached micrometer verniers was then used to examine the coating morphology and to make a quantitative determination of the severity of the corrosion attack utilizing the Aprigliano method. Depth of penetration measurements were taken at 400X magnification, every 20 degrees around the specimen circumference and numerically averaged. This representative value along with the maximum penetration depth reading were used to quantify the coating system performance as outlined in Tables V and VI.

After the optical evaluation was completed, the etchant film was removed with acetone and a thin conductive carbon overlay was deposited onto the surface of the formvar mount surrounding the specimen. A thin strip of colloidal silver paint connected the specimen surface to the carbon overlay to prevent excess static charge from accumulating on the specimen/mount interface during subsequent electron microscopy.

Scanning electron photomicrographs were taken of selected specimens in order to analyze coating microstructural features. These backscatter images, which can be found in Figures B.2 - B.25, show the coating structure prior to hot corrosion testing (as received) along with examples of typical surface pitting that resulted from the LTHC/HTHC attack. Lastly, continuous electron microprobe scans were made of the coatings in an attempt to characterize the reaction products present. This was done by determining the nickel, aluminum, platinum, chromium, titanium and molybdenum elemental weight percent concentrations as a function of distance transversed. Special effort was made to probe those "as received" specimens that were subjected to complex deposition treatments in order to detect any unexpected changes in element distributions that had occurred. Plots of the microprobe scan data can also be found in Figures B.2 - B.25.

IV. DISCUSSION AND RESULTS

The two nickel-based superalloy substrates selected for use in this investigation were IN-100 (10% chromium) and IN-738 (16% chromium). Their nominal weight percent compositions are delineated within Tables II and III respectively. A complete description of the coating formation processes/deposition parameters that were utilized are listed within Table IV. Electron microprobe results and SEM photomicrographs of selected specimens are also presented in Figures B.2 - B.25. Unfortunately, exact phase identification was not always possible in this investigation due to the lack of appropriate phase diagrams within the literature and an absence of X-ray diffraction data.

A. COATING STRUCTURE MORPHOLOGY

The "as received" test specimens that were evaluated under hot corrosion conditions can be categorized structurally as follows:

1. Uncoated Substrate

As previously discussed, the principle difference between the two superalloys employed in this study was their chromium content and hence their inherent hot corrosion resistance. The IN-738 microprobe data presented in Figure B.2(b) confirms its elemental composition. When placed in a LTHC environment, selective grain boundary attack appeared

to dominate as shown in Figure B.3(a). This type of attack was rather surprising as the more conventional LTHC attack morphology (i.e., localized pitting) had been expected.

2. LTHA Diffusion Aluminide (No Pt or Cr Additions)

Utilizing a high activity deposition process resulted in the typical three zone coating structure shown in Figure B.4(a). The outer zone carbide precipitates and the underlying "denuded zone" are readily apparent. Figure B.5(a) reveals the catastrophic nature of the LTHC attack mechanism and also shows the detached metal oxide reaction products which no longer afford protection to the underlying substrate.

3. HTLA Diffusion Aluminide (No Pt or Cr Additions)

This low aluminum activity deposition process produces an outward diffusion of nickel. A two zone coating results with a nickel-rich outer layer of β as verified by the microprobe scan data in Figure B.6(b). This outer layer of β is devoid of substrate element precipitates as expected. The initial surface is clearly marked by a series of substrate element precipitates slightly above the interdiffusion zone as seen in Figure B.6(a). Figure B.7(b) presents an excellent example of the rough, mottled morphology that is characteristic of the HTHC mode of attack.

4. LTHA Chromium-Modified Aluminide (No Pt Addition)

This coating, formed by an inward diffusion of aluminum on a chromium enriched surface, produced the standard three zone structure presented in Figure B.8(a). The outer zone is fully enriched with chromium as confirmed by the microprobe scan data within Figure B.8(b). Excess chromium precipitates out as a fine assemblage of second phase α-Cr as exhibited by the small, light colored dots within the outer zone of Figure B.8(a). An intermediate zone of β denuded of substrate element precipitates is also readily apparent. Figure B.9(a) clearly illustrates the localized pitting that is characteristic of the LTHC degradation mechanism.

5. HTLA Chromium-Modified Aluminide (No Pt Addition)

This two zone outward coating consists of an outer layer of phase pure β, with substrate elements that have diffused out concurrently with the nickel, forming precipitates. Much of the chromium is also in the form of precipitates and is located within the inner regions of the coating structure, near the interdiffusion zone. This internal concentration of chromium is confirmed by the microprobe scan plot of Figure B.10(b).

6. LTHA Platinum-Aluminide (No Cr Addition)

This inward type platinum-modified aluminide develops the four zone structure previously discussed. The light colored surface zone of Figure B.14(a) is

predominantly a platinum-rich layer of $PtAl_2$. Below that, in the outer intermediate zone, a fine distribution of platinum-rich precipitates are contained within an aluminum enriched NiAl matrix. The inner intermediate zone is denuded of any other phases or substrate element precipitates as expected. Figures B.13(a) and B.15(a) present some excellent examples of localized LTHC pitting attack where the outer $PtAl_2$ layer is left essentially intact. Figure B.15(b) displays the characteristic HTHC attack morphology which contrasts markedly from the LTHC pitting of Figures B.13(a) and B.15(a).

7. ITIA Platinum-Aluminide (No Cr Addition)

This intermediate temperature, intermediate activity process produced the three zone coating structure of Figure B.16(a). The outer zone is composed of a platinum-rich $PtAl_2$ phase within an NiAl matrix. The intermediate zone is essentially β with a lean distribution of insoluble substrate element precipitates and carbides located near the interdiffusion zone. Figure B.17(a) illustrates the selected undercutting that often develops as part of the LTHC attack mechanism.

8. HTLA Platinum-Aluminide (No Cr Addition)

The longer pre-diffusion heat treatment used with this outward coating produced a two phase, three zone structure as shown in Figure B.18(a). The surface zone consists of a non-continuous layer of platinum-rich $PtAl_2$

precipitates contained within an aluminum-rich NiAl matrix. The intermediate zone is a single phase of β, rich in nickel as a result of its outward diffusion. The inner zone is again an interdiffusion zone consisting primarily of refractory metal-rich phases and carbides within an NiAl matrix.

9. Pt + (Cr + Al) - Single Step

The chromium modified platinum-aluminides have structures that are more complex as a result of the addition of a second modifying element. The paucity of information within the literature concerning these types of coatings and the lack of X-ray diffraction data makes detailed phase identification extremely difficult. As shown in Figure B.20(a), a three zone coating structure has developed from this presumed high activity process. The outer zone appears to be composed of a platinum enriched phase (possibly $PtAl_2$) and chromium precipitates (probably α-Cr) dispersed within an NiAl matrix. Although the diffusion step includes both the deposition of Cr and Al sequentially in a single coating step, the level of chromium in the outer coating layer is only marginally higher than the standard ITIA aluminizing cycle. The inner coating layer probably consists of precipitates of both platinum and chromium contained within an NiAl matrix.

10. Process B (Pt + Cr + Al) - Two Step

This HTLA two step process produced a three zone structure which is quite similar to that of a standard HTLA platinum-aluminide. From Figures B.22(a) and (b), it can be established that the outermost zone is most likely a chromium-rich Pt-Al phase (probably $PtAl_2$) containing some nickel. This raises the possibility of some significant chromium solubility in $PtAl_2$, a situation not shown in presently available phase diagrams. In addition, some of the chromium at the surface is in the form of dispersed chromium-rich precipitates (α-Cr) generated by the chromizing process. Since this HTLA aluminizing step involves a vapor deposition process, no pack mix entrapment is possible. An intermediate layer of precipitate-free β appears as the denuded zone in Figure B.22(a). The interdiffusion zone primarily consists of chromium carbides within an NiAl matrix as previously seen and discussed.

11. Process D (Cr + Pt + Al) - Two Step

In this process sequence, the order in which the chromium and platinum are applied has reversed. This results in a three plus zone structure not typical for most aluminides or modified aluminides. As shown in Figure B.23(a), a relatively thick layer of platinum-rich $PtAl_2$ appears on the coating surface. The intermediate zone is most likely a matrix of β with an increasing concentration of α-Cr and other substrate element-rich precipitates. The

interdiffusion zone again consists of chromium and refractory metal carbides within an NiAl matrix. This coating structure appears to combine the effects of the inward and outward diffusion processes as its structure possess attributes of both. In practice, while it is relatively easy to control the aluminizing process in either the high activity or low activity region of β, the region where both Al and Ni are mobile with comparable diffusivities is very limited and difficult to manage. Apparently, the presence of chromium enrichment and the platinum serves to produce an aluminizing process where this condition occurs.

B. LOW TEMPERATURE HOT CORROSION TEST RESULTS

From the LTHC test data presented in Table V, it is readily apparent that the most resistant coatings against LTHC attack were the HTLA/ITIA platinum-aluminides and the Process D (Cr + Pt + Al) coating. These coating structures improved hot corrosion resistance regardless of which substrate was used. This enhanced LTHC protectivity can undoubtably be attributed to the high density of $PtAl_2$ at or near the coating surface. Underneath the primary $PtAl_2$ surface layer was a thick two-phase zone of $PtAl_2$ within an NiAl matrix. After the initial $PtAl_2$ surface layer was penetrated, it appears that the $PtAl_2$ precipitates and some α-Cr afforded further hot corrosion protection. The LTHA platinum-aluminides, on the other hand, were not quite as

effective. Although this coating structure possesses a thin surface layer of $PtAl_2$, which does improve LTHC performance over the unmodified aluminides, once this barrier was breached, the corrosion attack proceeded rapidly as demonstrated in Figure B.13(a). This is to be expected from a LTHA inward type coating which concentrates substrate elements within the outer zone of the coating as opposed to the HTLA outward type which has a surface zone relatively free of substrate strengthening elements such as the refractory metals. In general, the platinum aluminide test results confirm the general consensus found within the literature, i.e., a thick, continuous surface layer of $PtAl_2$ is the most resistant LTHC structure.

The chromium-aluminides were not quite as effective as the $PtAl_2$ forming platinum-aluminides in enhancing LTHC protectivity. The reason for this appears to be tied to the amount of chromium (and its morphology) actually present near the coating surface. For the LTHA chromium-aluminides, a relatively high surface chromium enrichment resulted in a more resistant surface structure than the unmodified aluminides or the HTLA chromium-aluminides which had minimum chromium in the outer zone. The HTLA (outward type) chromium aluminide, on the other hand, had a higher chromium concentration near the interdiffusion zone as might be expected. This produced a coating structure that offered little initial LTHC resistance but effectively slowed

corrosion penetration once the chromium enriched interdiffusion zone was reached. These localized chromium concentrations are substantiated by the microprobe data presented in Figures B.8(b) and B.10(b). It is interesting to note that for the low temperature hot corrosion testing, even the best alumina formers still only produced a two-fold increase in overall LTHC performance.

The three chromium modified platinum-aluminides tested in this study varied greatly in their LTHC resistance. Of these three coating systems, the Process D coating (Cr + Pt + Al) performed best overall. By applying chromium first and then platinum prior to aluminizing, a thick protective layer of $PtAl_2$ formed on the surface as shown in Figure B.24(a). Supporting the $PtAl_2$ surface layer, is a profuse second phase of α-Cr within the underlying intermediate zone. This sequential arrangement of protective layers (i.e., $PtAl_2$ then α-Cr) combined to make the Process D coating beneficial, not only for LTHC resistance, but HTHC as well.

The Pt + (Cr + Al) - one step process only furnished moderate LTHC resistance primarily because of its relatively low surface chromium content. As shown in Figure B.20(b), the concentration of chromium is low at the coating surface but rises dramatically as the interdiffusion zone is approached. This would account for its moderate overall LTHC resistance and relatively low maximum depth of

penetration. The corrosion attack proceeds rapidly through the outer coating regions composed principally of NiAl, but slows considerably once the zone of high chromium content is reached.

The Process B coating (Pt + Cr + Al), which provided the least LTHC resistance, had a discontinuous surface layer of $PtAl_2$ with high amounts of nickel (probably NiAl) and some chromium. This sequence of modifying element additions (i.e., Pt first, then Cr) seems to have lowered the surface platinum content and adversely affected the final coating structure. Again it is the thickness and continuity of the $PtAl_2$ surface layer that has emerged as the most important factor for LTHC resistance.

Finally, LTHC performance appears to be related to the overall thickness of the coating structure developed. Figure B.26 presents the normalized average depth of penetration as a function of overall coating thickness. For the platinum-aluminides, the obvious trend is that LTHC resistance varies directly with the overall coating thickness, or alternatively, as the coating thickness increased, average depth of penetration decreased. One possible explanation for this is the increased isolation from deleterious substrate elements that the thicker coatings provide. It is not surprising then to find that the Process D coating, which was one of the most resistant coatings, was also by far the thickest.

C. HIGH TEMPERATURE HOT CORROSION TEST RESULTS

In contrast to the two-fold increases in protectivity achieved during LTHC testing, several of these same coatings provided up to a ten-fold increase in HTHC resistance. From the relative rankings of HTHC performance presented in Table VI, the Process D coating and the HTLA/ITIA platinum-aluminides once again appear as the most resistant structures. The HTHC data reinforces the premise made earlier, that high levels of platinum at the coating surface (i.e., as $PtAl_2$) enhances overall hot corrosion resistance considerably. Chromium additions were not nearly as beneficial for the HTHC testing as they were in the low temperature regime. In fact the chromium-aluminides performed only slightly better overall than the unmodified aluminides as expected.

As observed in the LTHC testing, coatings with a continuous $PtAl_2$ surface layer experienced relatively high maximum depths of penetration. The initial HTHC resistance of $PtAl_2$ at the coating surface was excellent, however, once this layer was breached, the corrosion attack proceeded at a fairly rapid pace. This was in contrast to the unmodified aluminides which exhibited a more uniform corrosion front.

A HTHC coating thickness correlation also existed as illustrated in Figure B.27. The thicker coating structures were generally the ones that afforded the most HTHC resistance. A notable exception to this observed trend was

the thinner LTHA platinum-aluminides which formed a relatively thick layer of $PtAl_2$ at the coating surface. This anomaly only serves to reinforce the central premise of this investigation: platinum additions are beneficial to overall hot corrosion resistance, especially when appearing as a thick, continuous surface layer of $PtAl_2$.

V. CONCLUSIONS

Based on microstructural analyses of the as-received coated specimens and the depth of penetration results from the LTHC/HTHC experimental runs, the following conclusions have been formulated:

1. Both Type 1 and Type 2 hot corrosion morphologies can be effectively reproduced by the laboratory furnace test rig assembled at the Naval Postgraduate School. This relatively inexpensive method serves as a useful screening device for obtaining a preliminary ranking of coating structures and materials, as well as for establishing archetype degradation morphologies for mechanistic studies.
2. A significant thickness effect exists for both platinum-modified and chromium-modified coatings. In general for the platinum-modified aluminides, thick, two-phase coatings displayed a greater propensity to resist the LTHC/HTHC fluxing mechanisms than thin, one-phase coatings. A notable exception to this occurred when a continuous single phase of $PtAl_2$ formed at the coating surface.
3. Differences in the substrate material's inherent corrosion resistance (i.e., IN-100 in lieu of IN-738) had little effect on the coating structure or the mean

depth of corrosion attack. Pre-existing surface flaws in the coating structure, on the other hand, appeared to be a much more significant variable and were found to be especially detrimental to LTHC protectivity behavior.

4. Coatings formed by an outward, low aluminum activity (HTLA) process exhibited improved hot corrosion performance over those produced utilizing an inward, high activity (LTHA) process.

5. Chromium substantially improves LTHC resistance when present in abundance at or near the coating surface. This enhanced protectivity can also be achieved with a chromium reservoir located within an internal layer of the coating provided pits on the order of 1.5 mils can be tolerated.

6. The presence of platinum concentrated near the coating surface markedly improves the HTHC resistance of diffusion aluminide coatings. LTHC performance, on the other hand, was not influenced as significantly by platinum additions, although, in some cases (i.e., when a continuous $PtAl_2$ surface layer exists) substantial improvement was noted.

7. Platinum-modified aluminide coatings can exhibit a wide range of structural variations depending primarily upon the pre-aluminizing diffusion treatment and the aluminizing process employed.

8. Platinum additions prior to the aluminizing step, significantly reduced the emergence of deleterious refractory metal precipitates within the outer regions of the coating structure.
9. All of the Pt-Al structures examined were found to be outstanding alumina formers. Additionally, the alumina adherence was excellent. However, once this layer was breached, the rate of corrosion attack equaled that of the unmodified aluminides.
10. Modifying the standard aluminide with both Cr and Pt can be beneficial when the deposition sequence results in a structure consisting of a continuous $PtAl_2$ outer layer supported by an inner layer containing a high chromium content. This Cr-Pt-Al deposition sequence seems to be especially beneficial for LTHC resistance when a HTLA aluminizing step is utilized. In some cases (i.e., when platinum is applied first, then chromium) it appeared that the chromium addition actually disrupted, or interfered with, the beneficial effects of the platinum.
11. Coated IN-100 test pins experienced a selected undercutting at their uncoated ends during HTHC testing and therefore were not included in this research.

This investigation was an initial attempt to gain some insight into the overall hot corrosion resistance of some of

the more promising coating system combinations currently being applied to nickel-based superalloy substrates. The following recommendations are offered for future research in order to better understand these coating structures and the factors affecting their performance:

1. An Energy-Dispersion X-ray Analysis should be performed on the coated specimens employed in this study. This EDAX testing would complement the electron microprobe scans in identifying specific phases present and the key diffusion mechanisms in effect.
2. Expand testing to include LTHA chromium-modified platinum aluminides for comparison with Process D coating structures. This study should be limited to coatings of similar thicknesses in order to remove this parameter variation and derive a more precise indication of coating system performance.
3. In this investigation, observed trends and conclusions were based upon the results of a limited number of test specimens. In future studies, it would be advantageous to conduct multiple sample testing of these same coated specimens in order to reduce statistical scatter/error and be able to assemble a more comprehensive data base.

APPENDIX A: TABLES I-VI

TABLE I

SUMMARY OF HOT CORROSION MECHANISMS

Possible Propagation Modes for Hot Corrosion of Superalloys by Na_2SO_4 Deposits

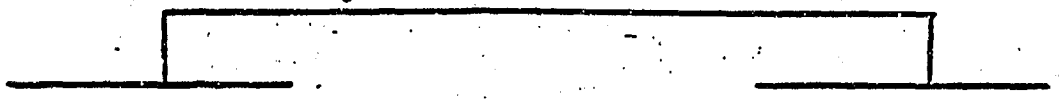

I. Modes Involving Fluxing Reactions
- Basic
- Acidic

II. Modes Involving A Component of the Deposit
- Sulfur
- Chlorine

I. Fluxing Modes

A. Basic Processes

1. Dissolution of Reaction Product Barriers, (i.e. AO) Due to Removal of Sulfur and Oxygen from the Na_2SO_4 by the Metal or Alloy:

SO_4^{2-} (sulfate deposit) → 1/2 S_2 (for reaction with alloy) + 3/2 O_2 (for reaction with alloy) + O^{2-} (for reaction with AO)

Reaction between AO and oxide ions can follow 2 courses:

(a) Continuous dissolution of AO

$$A(alloy) + 1/2\ O_2 + O^{2-} \rightarrow AO_2^{2-}$$

Na_2SO_4 is converted to Na_2AO_2 and attack is dependent on amount of Na_2SO_4 initially present.

(b) Solution and reprecipitation

$$A(alloy) + 1/2\ O_2 + O^{2-} \rightarrow AO_2^{2-}(solution) \rightarrow AO(precipitate) + O^{2-}$$

A supply of SO_3 is required in order for attack to proceed indefinitely, otherwise attack will stop when melt becomes sufficiently basic at precipitation site.

TABLE I
Summary of Hot Corrosion Mechanisms (con't)

B. Acidic Processes

1. Gas Phase Induced

(a) Formation of ASO_4 in Na_2SO_4:

$$A(alloy) + SO_3 + 1/2\ O_2 \rightarrow A^{2+} + SO_4^{2-}$$

Continuous solution of ASO_4 in Na_2SO_4 requires continuo. supply of SO_3 and O_2 from gas.

(b) Solution and Precipitation of AO in Na_2SO_4 Due to Reduction of SO_3:

$$A(alloy) + SO_3\ (from\ gas) \rightarrow A^{2+} + SO_3^{2-}\ (in\ melt)$$

$$A^{2+} + SO_3^{2-} + 1/2\ O_2\ (from\ gas) \rightarrow AO\ (precipitate) + SO_3$$

(c) Nonprotective Reaction Product Barrier formation due to rapid removal of base element (e.g. Co, Ni) from alloy by molten deposit (33).

(d) Solution and Precipitation of AO as a Result of Negative Gradient in Solubility of AO in Na_2SO_4 as in B.

2. Alloy Phase Induced

(a) Solution of AO in Na_2SO_4 Modified by Second Oxide from Alloy (i.e. BO_3).

Sequence:

i. Modification of Na_2SO_4 by BO_3

$$B(alloy) + 3/2\ O_2 + SO_4^{2-} \rightarrow BO_4^{2-} + SO_3$$

ii. Solution reaction for AO, Na_2SO_4 becomes enriched in ABO_4

$$A(alloy) + B(alloy + 2O_2 \rightarrow A^{2+} + BO_4^{2-}$$

or

iii. Solution and repricipitation

$$A(alloy) + B(alloy) + 2O_2 \rightarrow A^{2+} + BO_4^{2-} \rightarrow AO + BO_3$$

TABLE II

IN 100 CHEMICAL COMPOSITION

Element	Nominal Weight Percent
Ni	60.54
Cr	10.00
Co	15.00
Mo	3.00
Ti	4.70
Al	5.50
C	0.18
B	0.014
Zr	0.06
V	1.00

TABLE III

IN 738 CHEMICAL COMPOSITION

Element	Nominal Weight Percent
Ni	60.42
Cr	16.00
Co	8.50
Mo	1.75
W	2.60
Ti	3.40
Al	3.40
Nb	0.90
Ta	1.75
C	0.17
B	0.01
Zr	0.10
Fe	0.50 (max)
Mn	0.20 (max)
Si	0.30 (max)

TABLE IV

SUMMARY OF COATING DEPOSITION PROCESSES

Coating	Process
LTHA Diffusion Aluminide	1) Aluminizing - LTHA process* 2) Diffuse at 1080°C for 4 hours
HTLA Diffusion Aluminide	1) Aluminizing - HTLA process** 2) Diffuse at 1080°C for 4 hours
Process A	1) Platinizing - Electroplate 2) Aluminizing - HTLA process 3) Diffuse at 1080°C for 4 hours
LTHA Platinum - Aluminide	1) Platinizing - Electroplate 2) Diffuse at 870°C for ½ hour 3) Aluminizing - LTHA process 4) Diffuse at 1080°C for 4 hours
ITIA Platinum - Aluminide	1) Platinizing - Electroplate 2) Diffuse at 1050°C for 1 hour 3) Aluminizing - ITIA process*** 4) Diffuse at 980°C for 3.5 hours
HTLA Platinum - Aluminide	1) Platinizing - Electroplate 2) Diffuse at 870°C for 4 hours 3) Aluminizing - HTLA process 4) Diffuse at 1080°C for hours

*LTHA process in most industrial application involves chemical vapor deposition in the pack at approximately 760°C for 1 hour.

**HTLA process in most industrial applications involves chemical vapor deposition at 1020-1100°C for 3-8 hours. Specimens in this study were aluminized out of the pack.

***ITIA process in most industrial applications involves chemical vapor deposition at 850°C for 2-4 hours in a halide-free Al vapor.

TABLE IV

Summary of Coating Deposition Processes (cont'd.)

Coating	Process
LTHA Chromium - Aluminide	1) Chromizing - Pack Cementation at 1060°C for 7 hours 2) Aluminizing - LTHA process* 3) Diffuse at 1080°C for 4 hours
HTLA Chromium - Aluminide	1) Chromizing - Pack Cementation at 1060°C for 7 hours 2) Aluminizing - HTLA process** 3) Diffuse at 1080°C for 4 hours
Pt + Cr + Al (Single Step)	1) Platinizing - Electroplate 2) Chromize and Aluminize Sequentially in a Single Step Process 3) Diffuse at 1080°C for 4 hours
Pt + Cr + Al (2 Step) Process B	1) Platinizing - Electroplate 2) Chromizing - Pack Cementation at 1060°C for 7 hours 3) Aluminizing - HTLA process 4) Diffuse at 1080°C for 4 hours
Cr + Pt + Al (2 Step) Process D	1) Chromizing - Pack Cementation at 1060°C for 7 hours 2) Platinizing - Electroplate 3) Aluminizing - HTLA process 4) Diffuse at 1080°C for 4 hours

*LTHA process in most industrial applications involves chemical vapor deposition in the pack at approximately 760°C for 1 hour.

**HTLA process in most industrial applications involves chemical vapor deposition at 1080°C for 4 hours. Specimens in this study were aluminized out of the pack.

TABLE V

RESULTS OF LTHC TESTING*

Specimen Identification		Average Depth of Penetration (microns)	Maximum Depth of Penetration (microns)	Initial Coating Thickness (microns)
Substrate	Coating			
IN 738	ITIA Platinum - Aluminide	31.0	55.5	66.2
IN 738	Process D (Cr + Pt + Al)	34.0	42.0	143.6
IN 738	Process A (HTLA Pt - Al)	36.0	48.5	67.7
IN 100	HTLA Platinum - Aluminide	37.0	50.0	86.2
IN 100	LTHA Chromium - Aluminide	38.0	51.5	80.0
IN 738	HTLA Diffusion Aluminide	39.4	44.0	50.8
IN 100	Pt + (Cr + Al) - 1 Step	42.2	46.5	52.3
IN 738	HTLA Chromium - Aluminide	46.0	54.5	66.2
IN 738	LTHA Platinum - Aluminide	46.4	56.0	60.0
IN 738	LTHA Diffusion Aluminide	48.0	64.5	73.8
IN 738	Process B (Pt + Cr + Al)	56.0	66.0	73.8
IN 738	Unmcoated	67.2	95.5	N/A
IN 100	Uncoated	87.1	105.0	N/A

* All LTHC testing conducted at 700°C for 100 hours

TABLE VI

RESULTS OF HTHC TESTING*

Specimen Identification		Average Depth of Penetration (microns)	Maximum Depth of Penetration (microns)	Initial Coating Thickness (microns)
Substrate	Coating			
IN 738	Process D (Cr + Pt + Al)	5.2	17.5	143.6
IN 738	ITIA Platinum - Aluminide	5.5	21.5	66.2
IN 738	Process B (Pt + Cr + Al)	6.1	15.5	73.8
IN 738	Process A (HTLA Pt - Al)	7.7	19.0	67.7
IN 738	LTHA Platinum - Aluminide	11.1	21.5	60.0
IN 738	LTHA Chromium - Aluminide	11.8	17.0	80.0
IN 738	LTHA Diffusion Aluminide	12.2	22.5	73.8
IN 738	Pt + (Cr + Al) - 1 Step	12.7	20.5	52.3
IN 738	HTLA Chromium - Aluminide	13.3	21.0	66.2
IN 738	HTLA Diffusion Aluminide	33.3	39.0	50.8
IN 738	Uncoated	46.2	62.0	N/A

* All HTHC testing conducted at 900°C for 200 hours

APPENDIX B: FIGURES B.1 - B.27

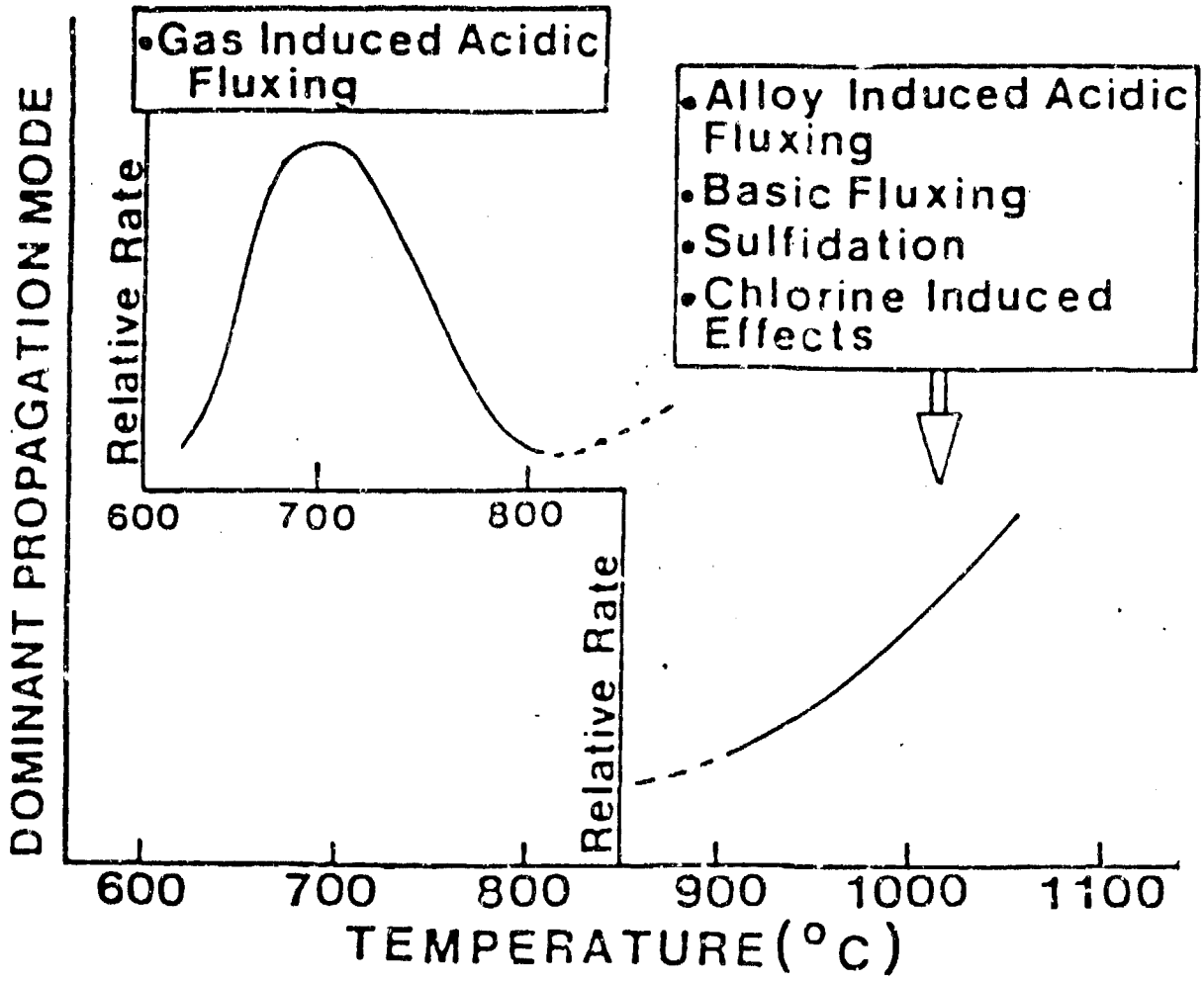

Figure B.1 Relative Rates of Hot Corrosion Attack

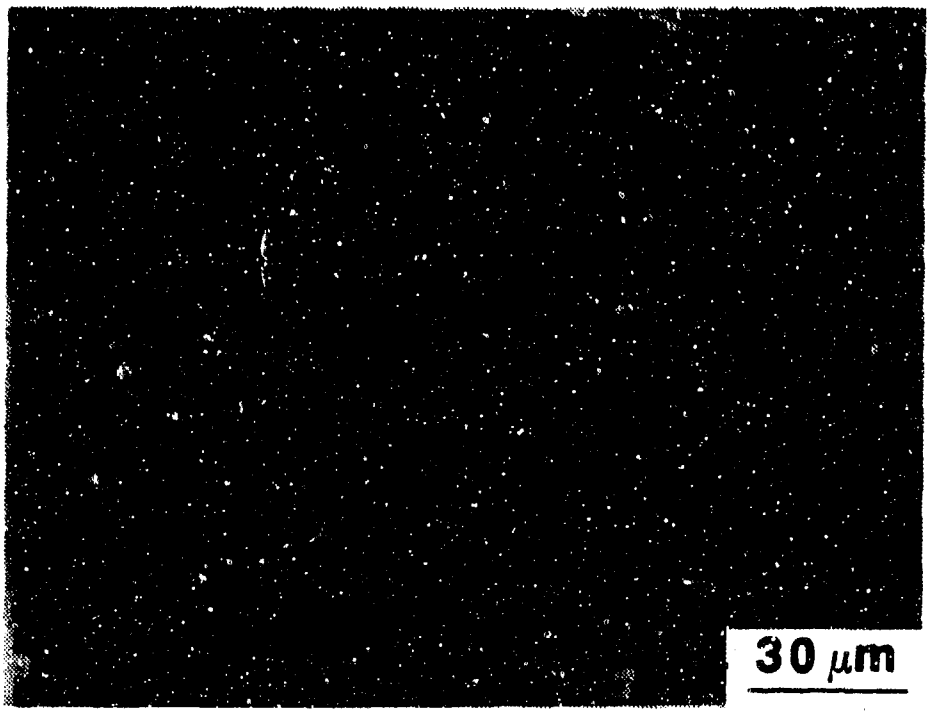

Figure B.2(a) Uncoated Substrate/IN-738 (as-received).

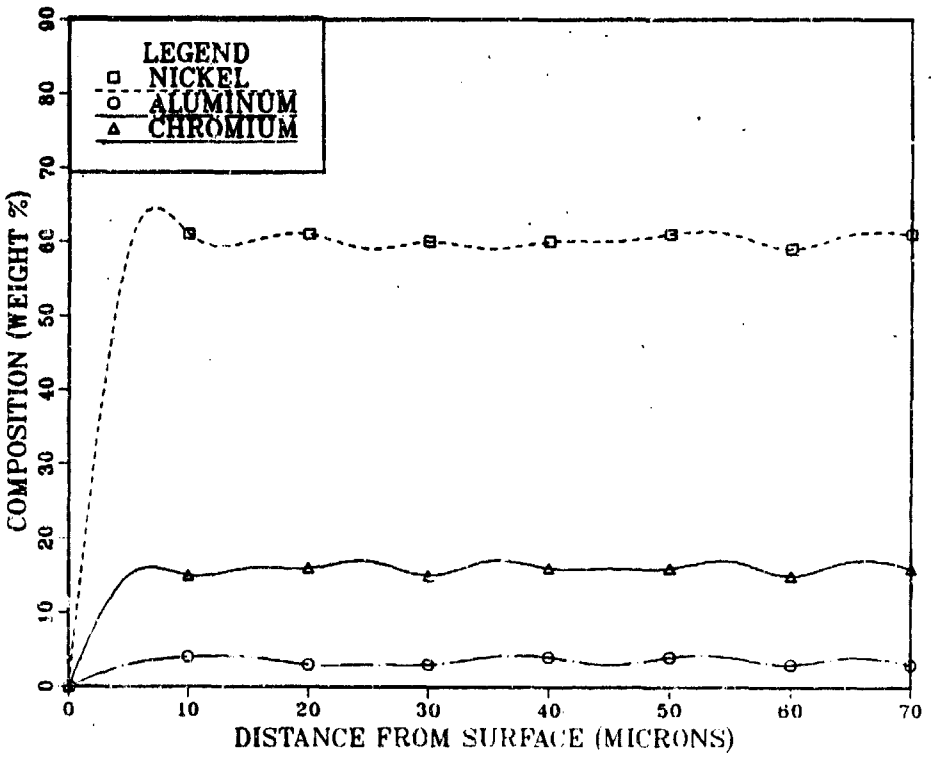

Figure B.2(b) Composition of Uncoated Substrate/IN-738.

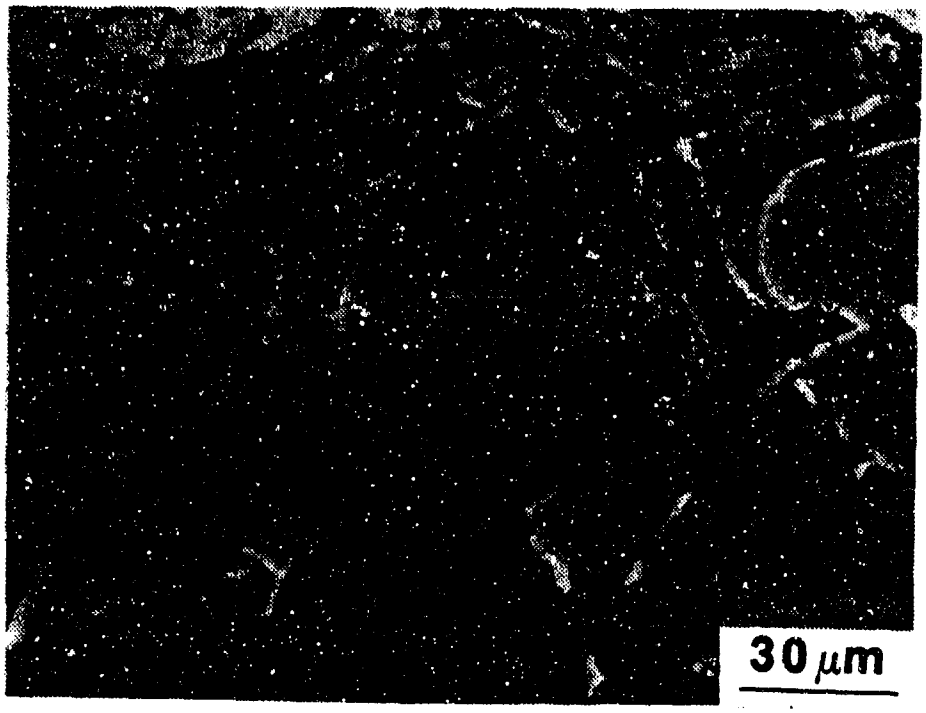

Figure B.3(a) Uncoated Substrate/IN-738 (LTHC-100 hrs).

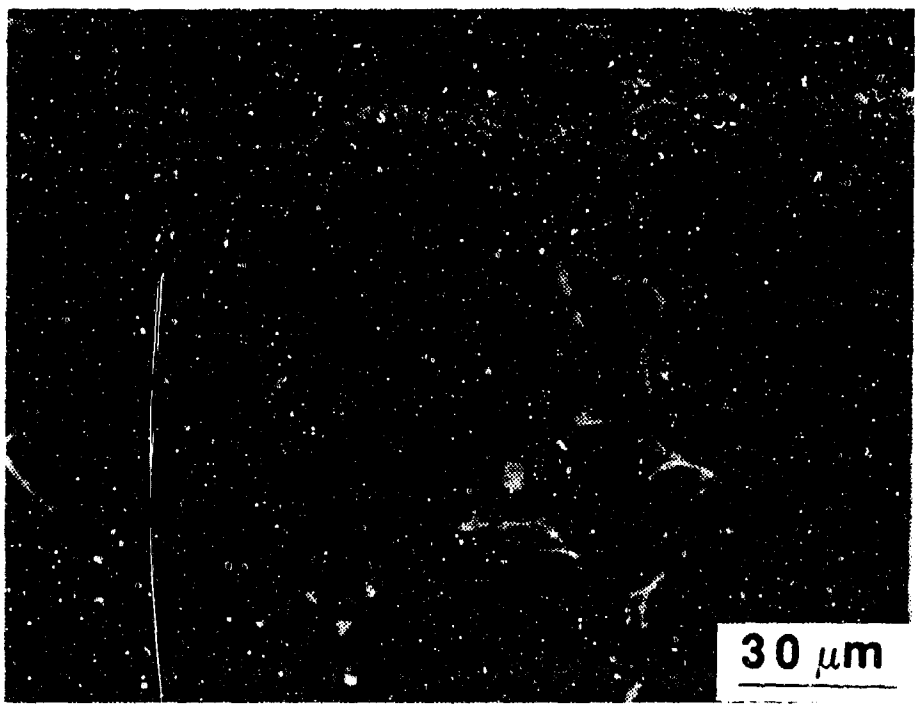

Figure B.3(b) Uncoated Substrate/IN-738 (HTHC-200 hrs).

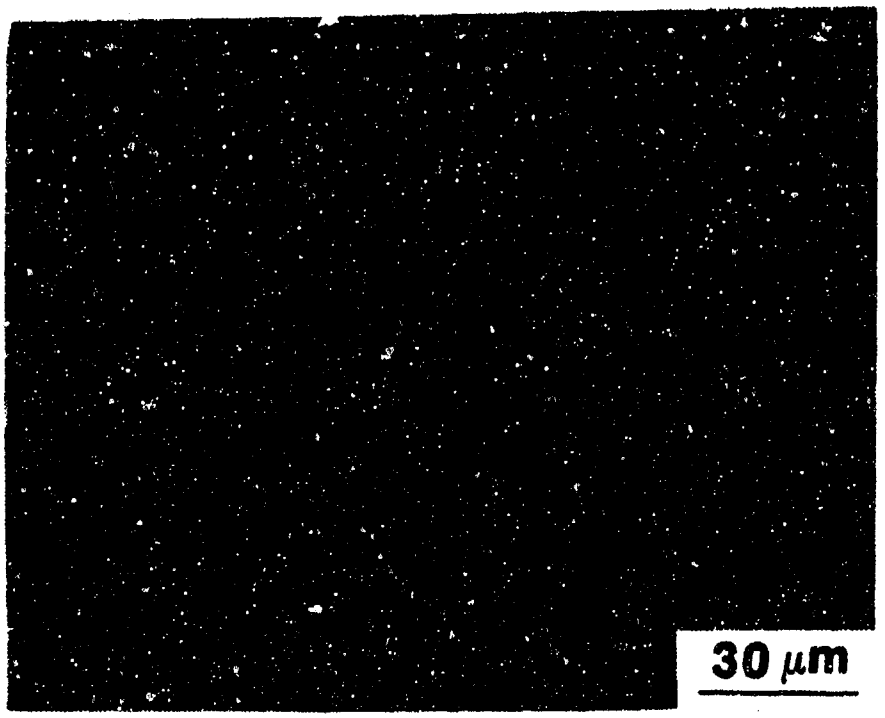

Figure B.4(a) LTHA Diffusion Aluminide/IN-100 (as-received).

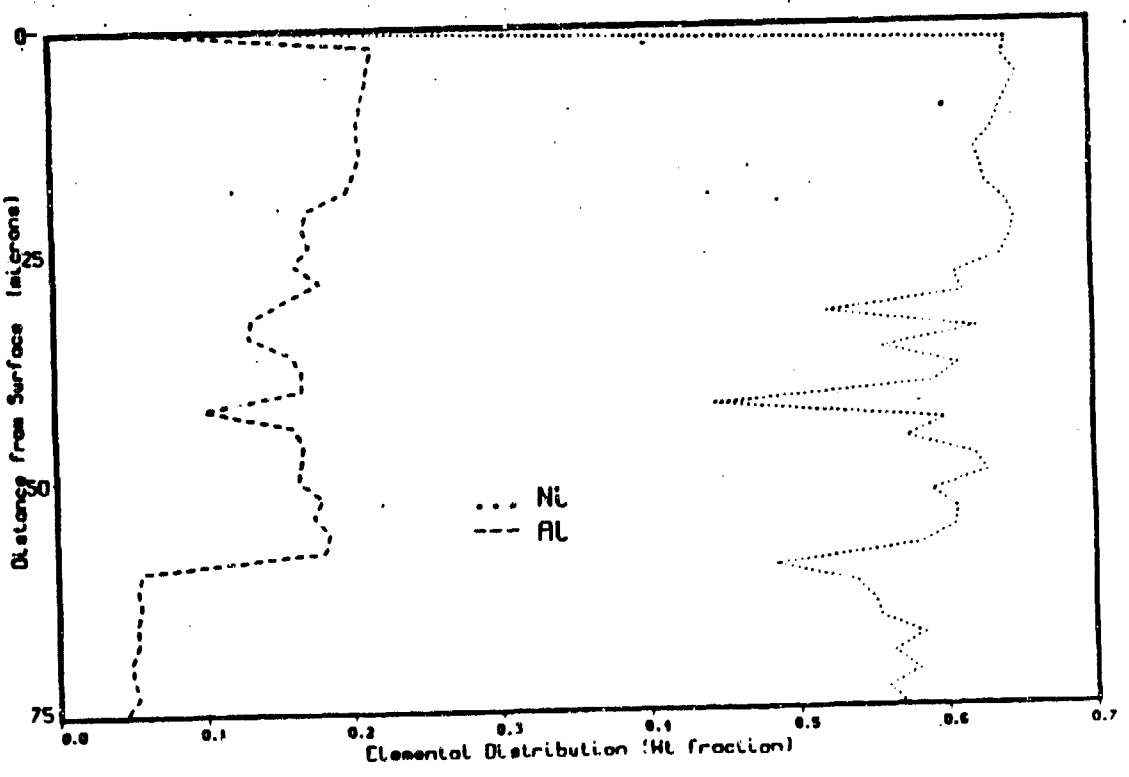

Figure B.4(b) Composition of LTHA Diffusion Aluminide/ IN-100.

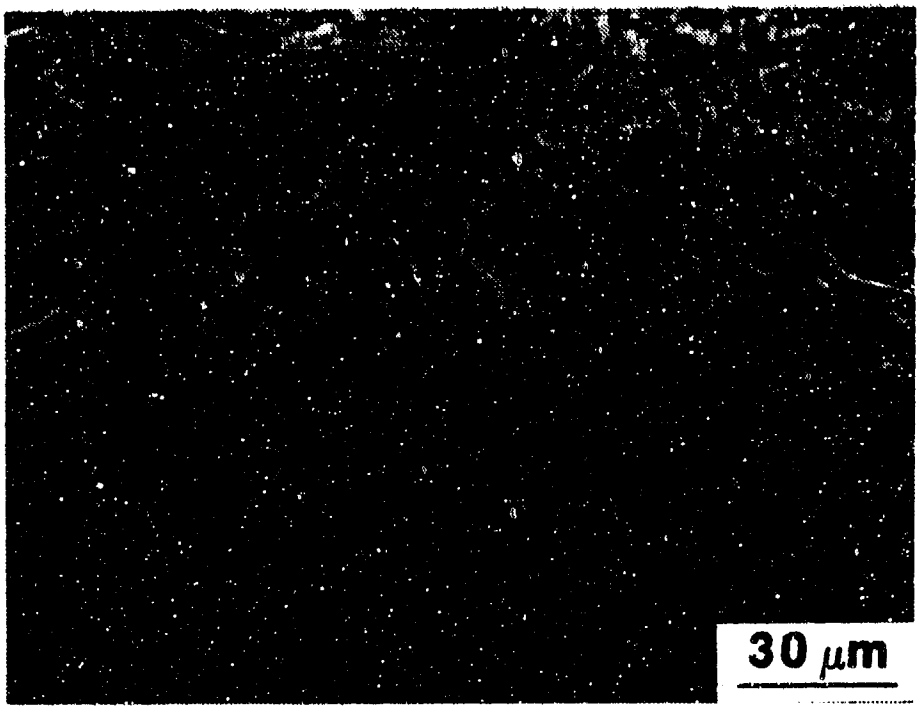

Figure B.5(a) LTHA Diffusion Aluminide/IN-100 (LTHC-100 hrs).

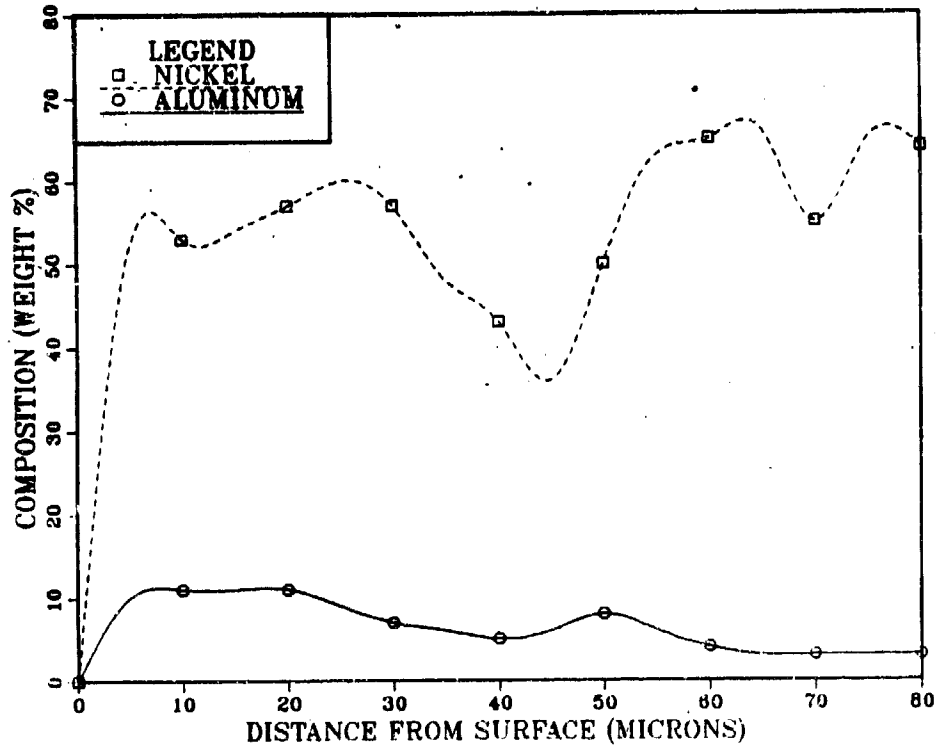

Figure B.5(b) Composition of LTHA Diffusion Aluminide/ IN-100 (LTHC-100 hrs).

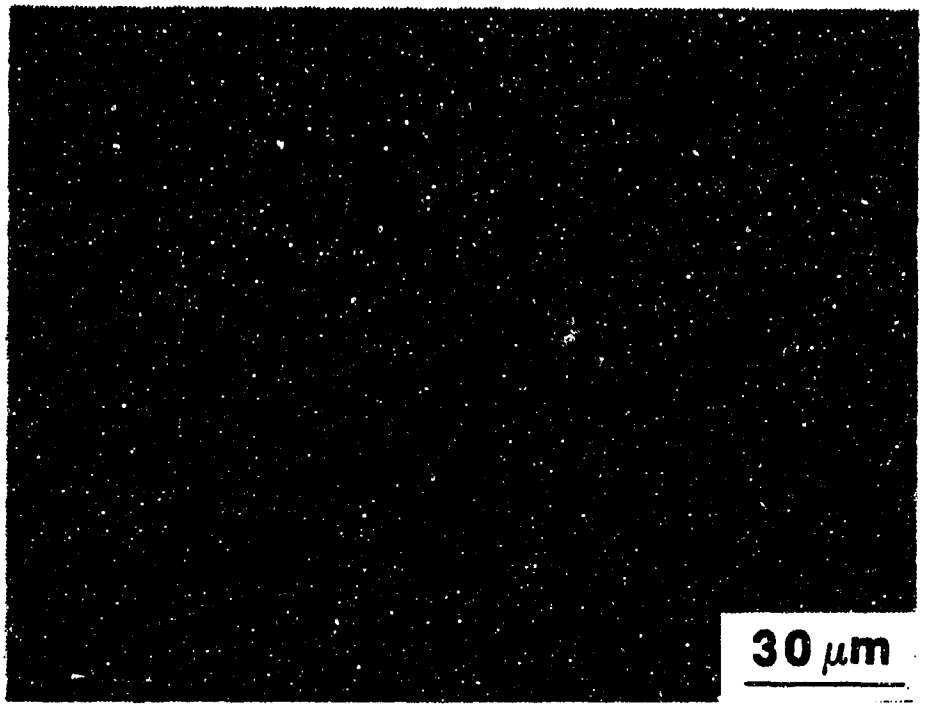

Figure B.6(a) HTLA Diffusion Aluminide/IN-738 (as-received).

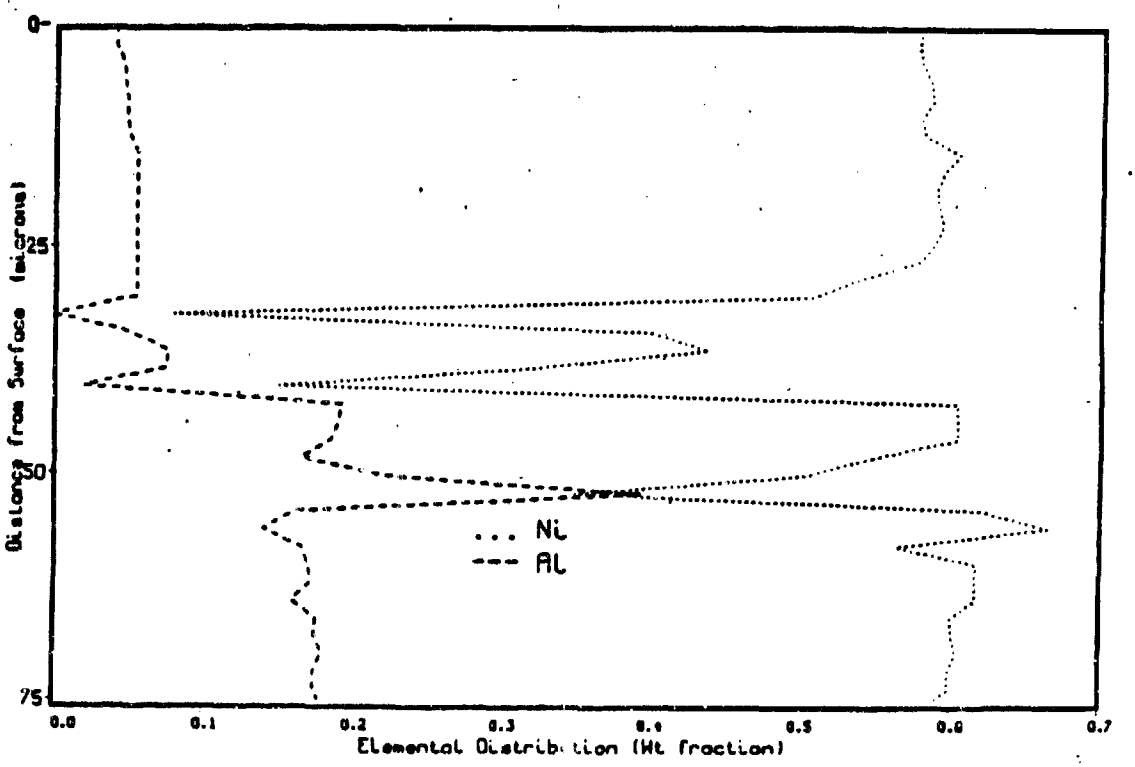

Figure B.6(b) Composition of HTLA Diffusion Aluminide/IN-738.

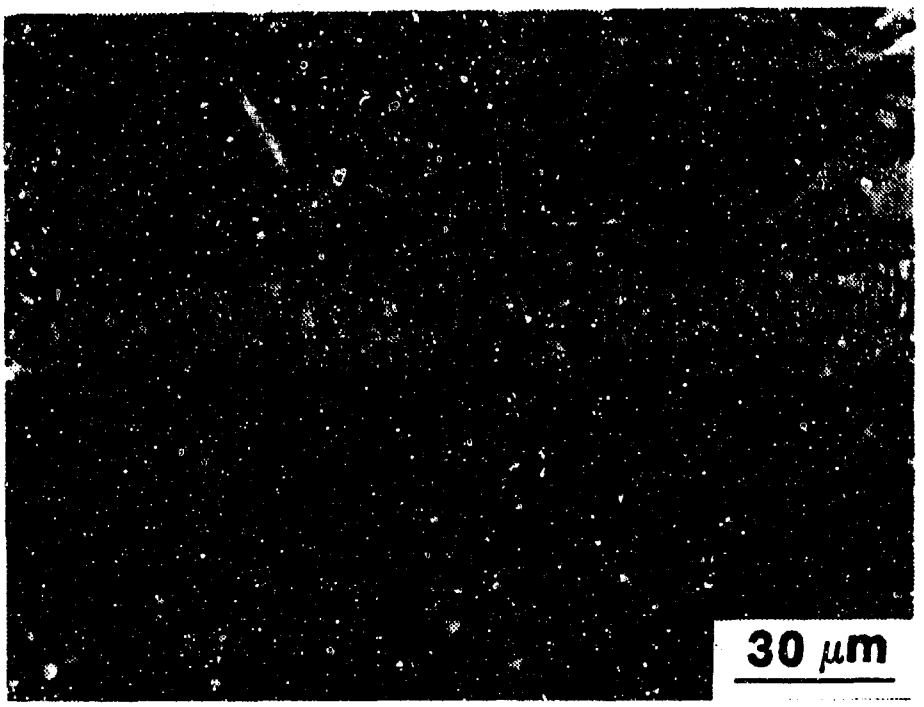

Figure B.7(a) HTLA Diffusion Aluminide/IN-738 (LTHC-100 hrs).

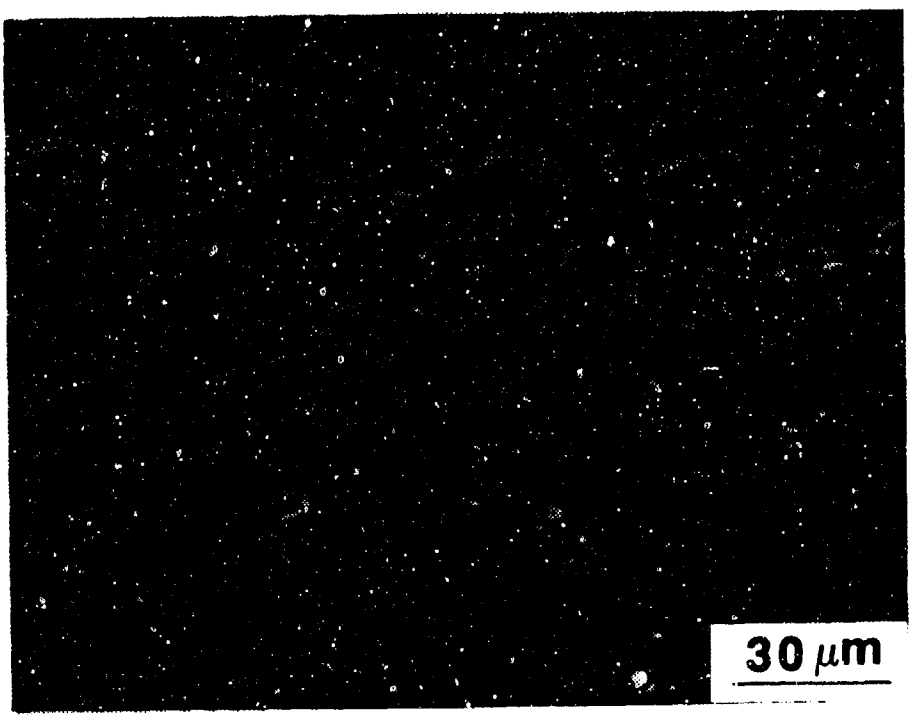

Figure B.7(b) HTLA Diffusion Aluminide/IN-738 (HTHC-200 hrs).

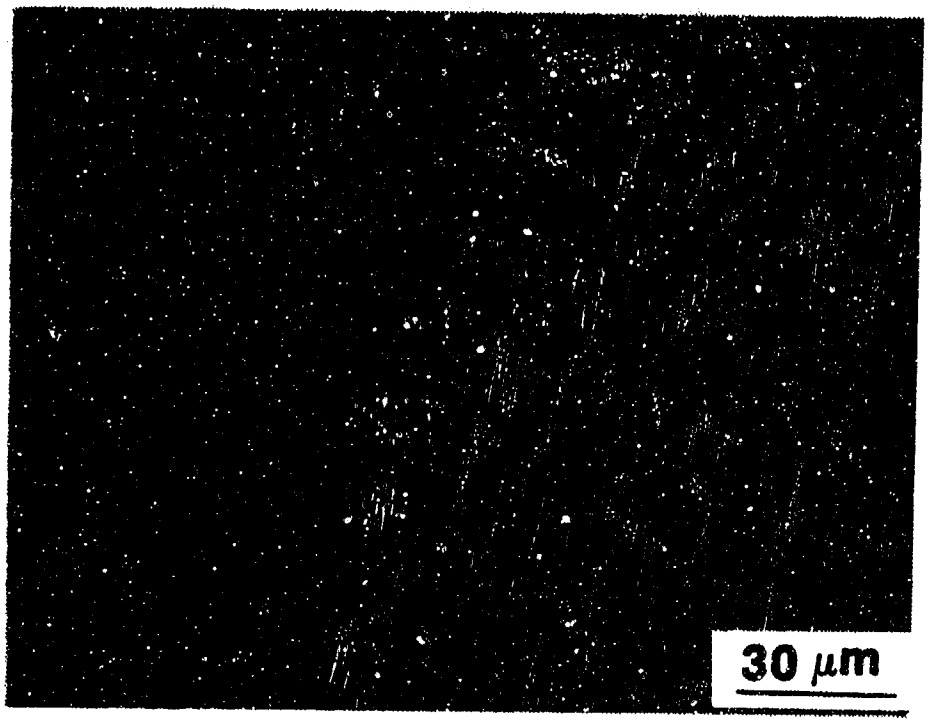

Figure B.8(a) LTHA Chromium-Aluminide/IN-738 (as received).

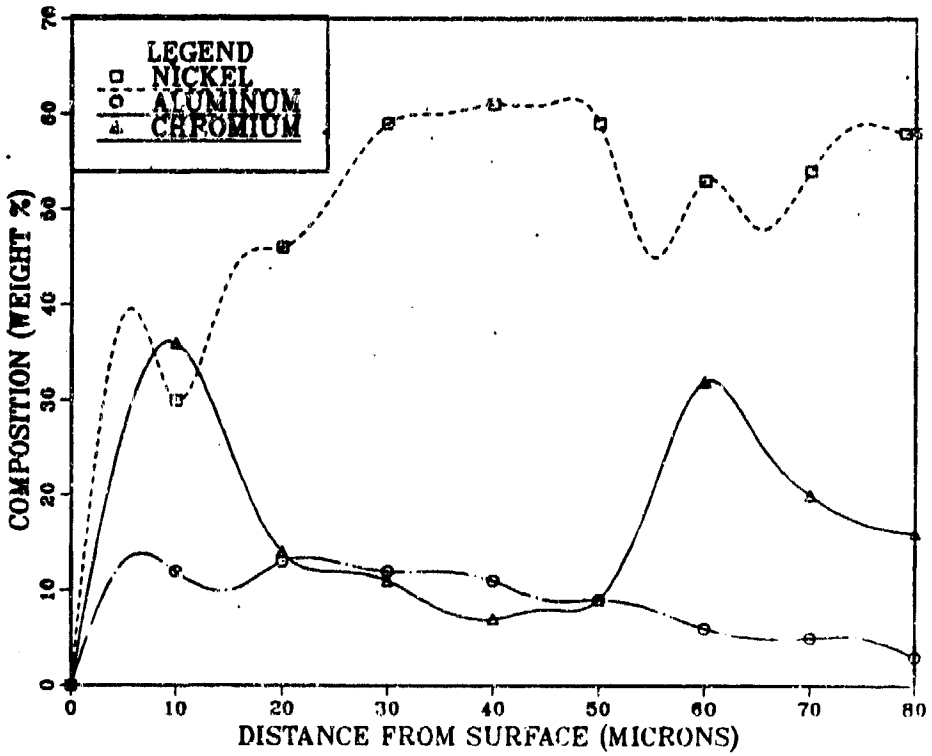

Figure B.8(b) Composition of LTHA Chromium-Aluminide/IN-738.

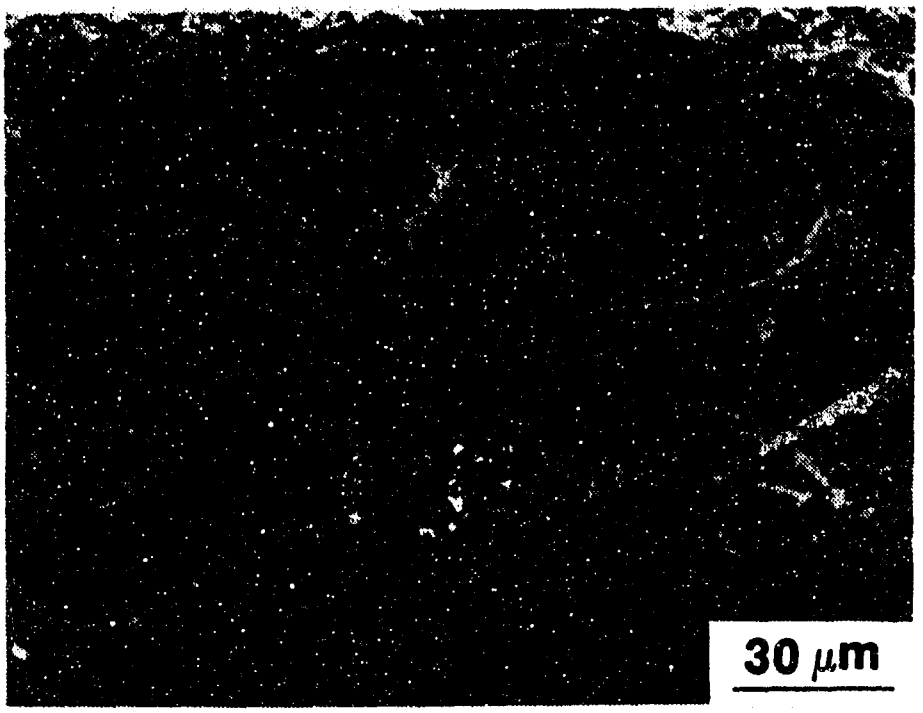

Figure B.9(a) LTHA Chromium-Aluminide/IN-738 (LTHC-100 hrs).

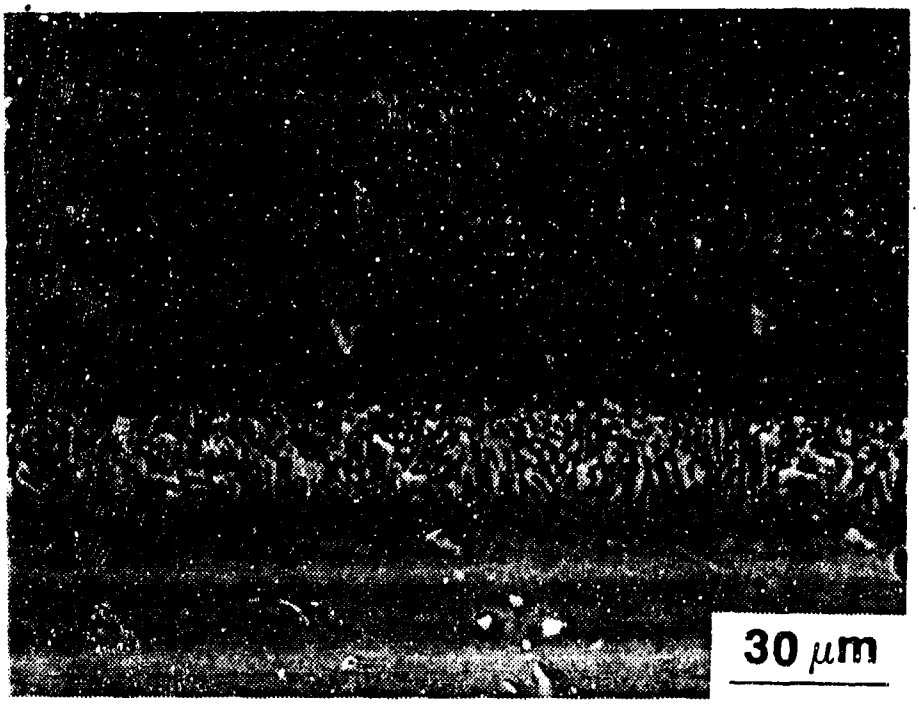

Figure B.9(b) LTHA Chromium-Aluminide/IN-738 (HTHC-200 hrs).

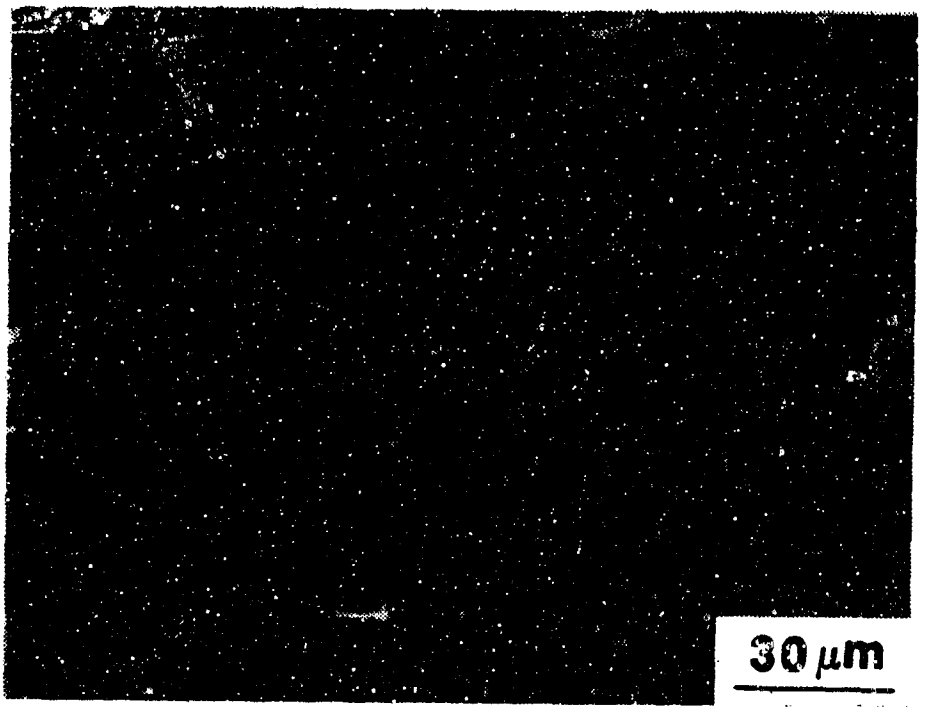

Figure B.10(a) HTLA Chromium-Aluminide/IN-738 (as-received).

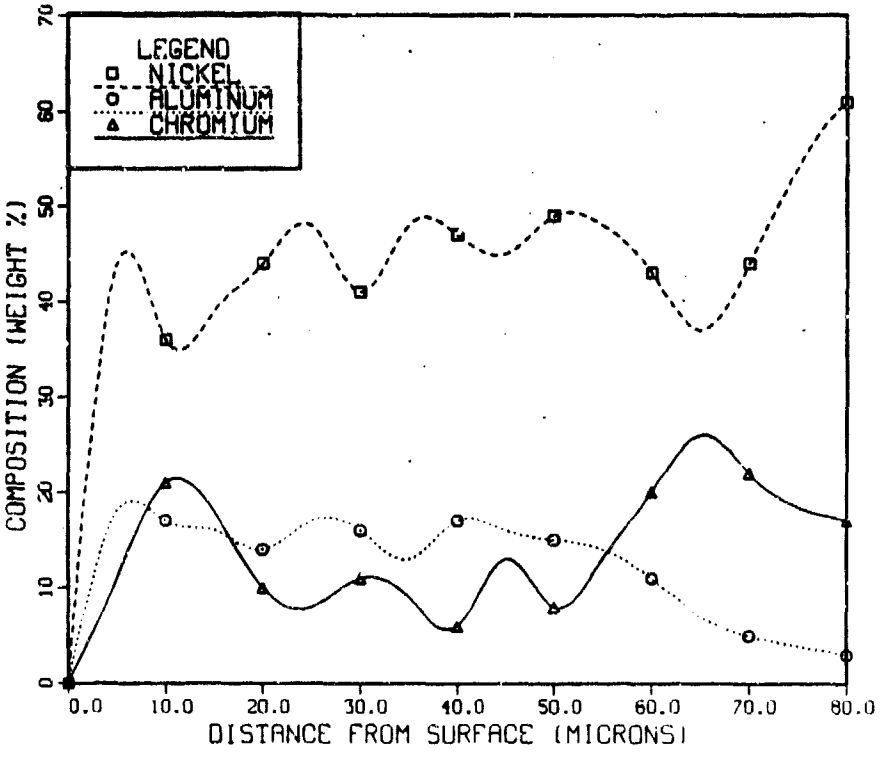

Figure B.10(b) Composition of HTLA Chromium-Aluminide/IN-738.

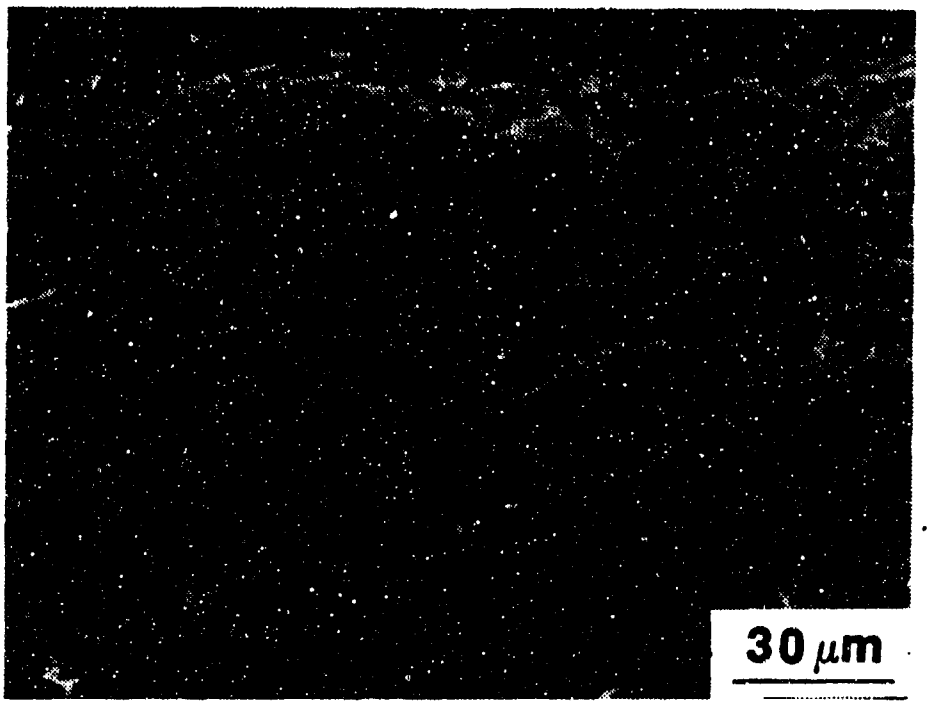

Figure B.11(a) HTLA Chromium-Aluminide/IN-738 (LTHC-100 hrs).

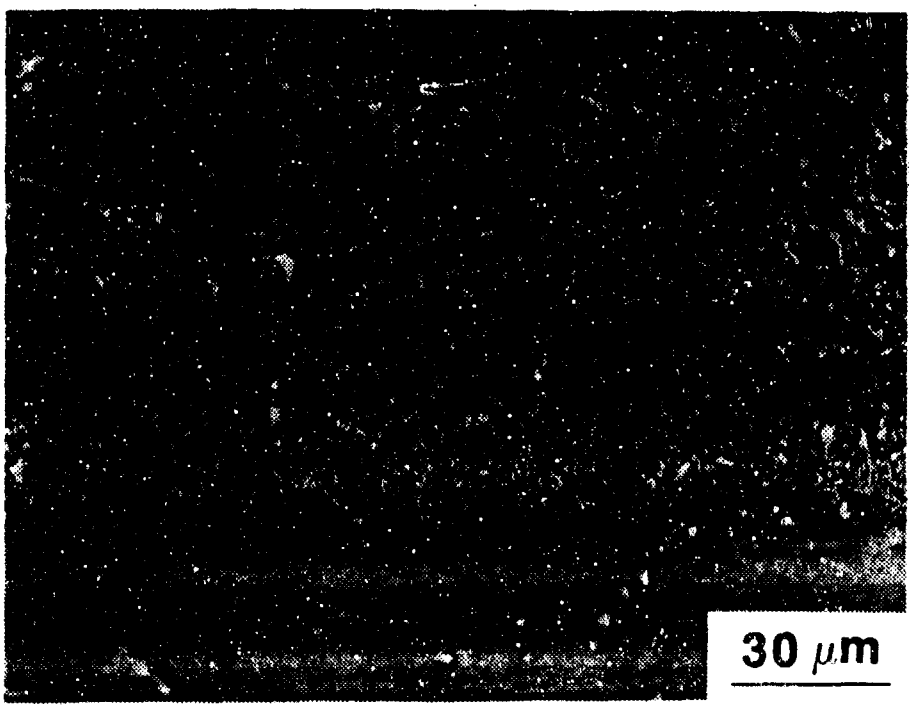

Figure B.11(b) HTLA Chromium-Aluminide/IN-738 (HTHC-200 hrs).

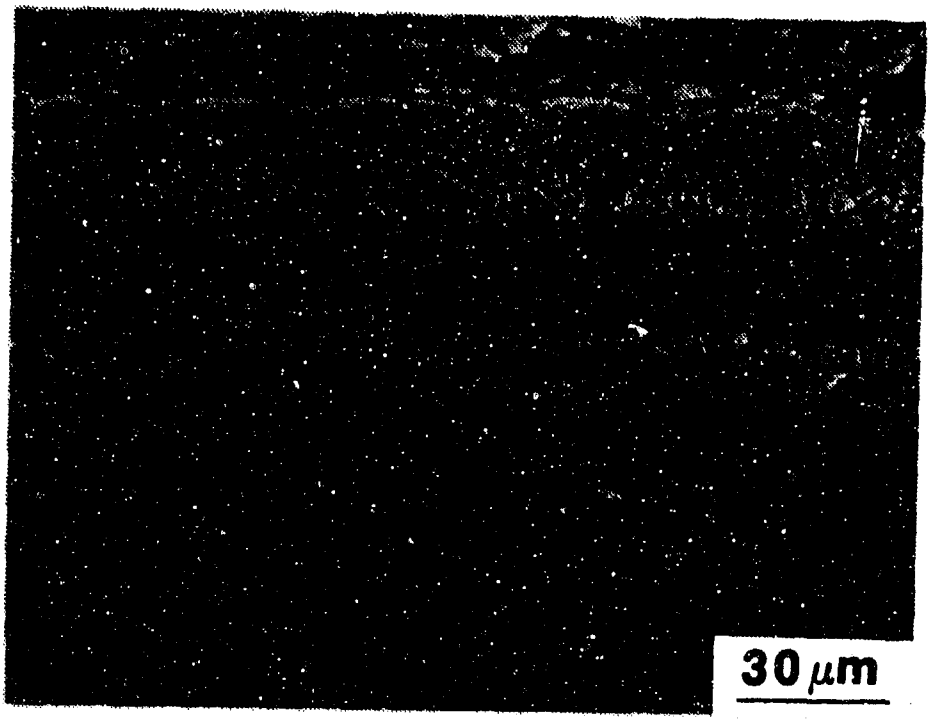

Figure B.12(a) LTHA Platinum-Aluminide/IN-738 (as-received). Pre-Aluminizing Diffusion Heat Treatment (1925°F/1hr)

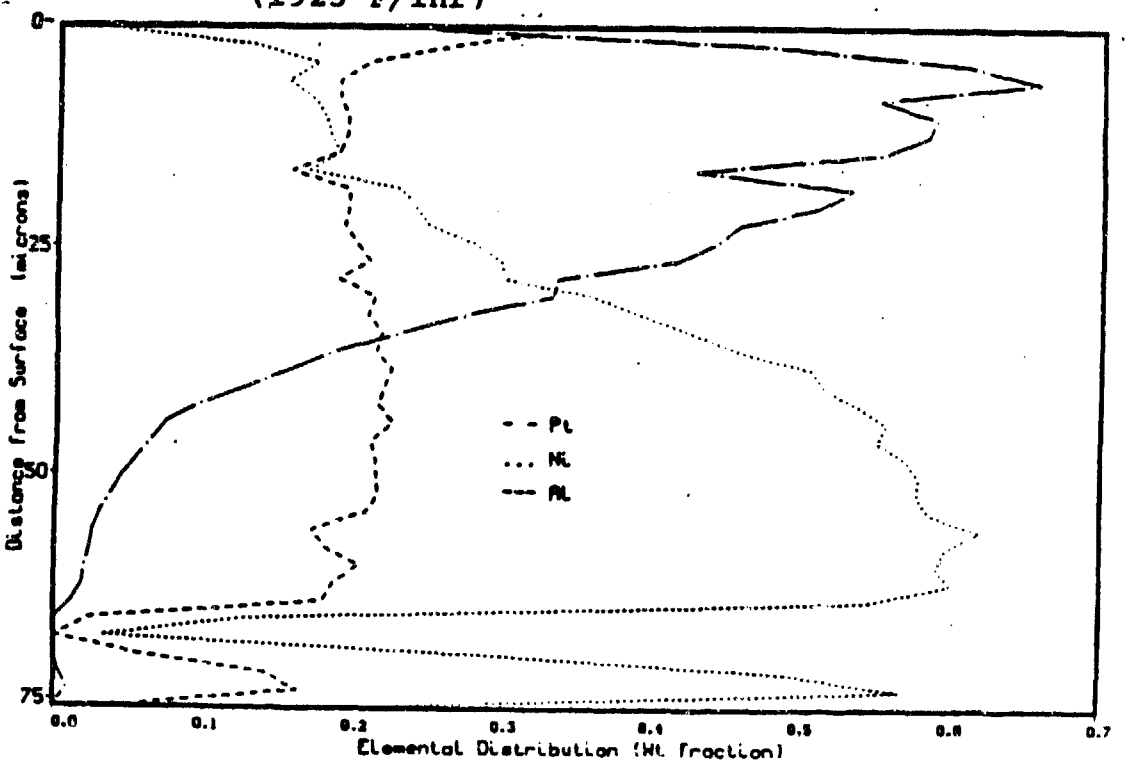

Figure B.12(b) Composition of LTHA Platinum-Aluminide/IN-738. Pre-Aluminizing Diffusion Heat Treatment (1925°F/1hr)

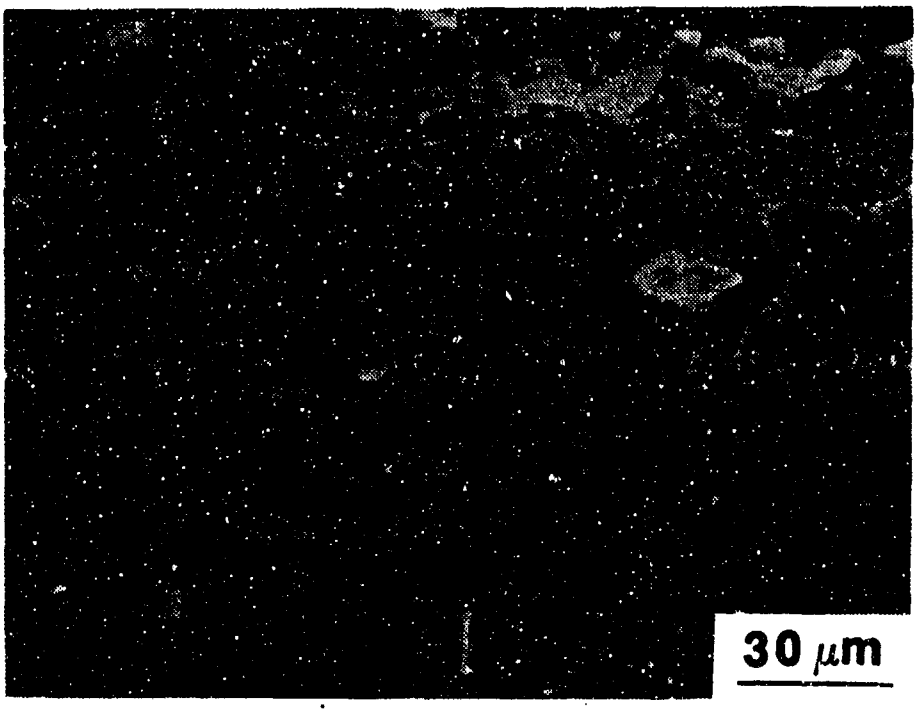

Figure B.13(a) LTHA Platinum-Aluminide/IN-738 (LTHC-100 hrs). Pre-Aluminizing Deffusion Heat Treatment (1925°F/1hr)

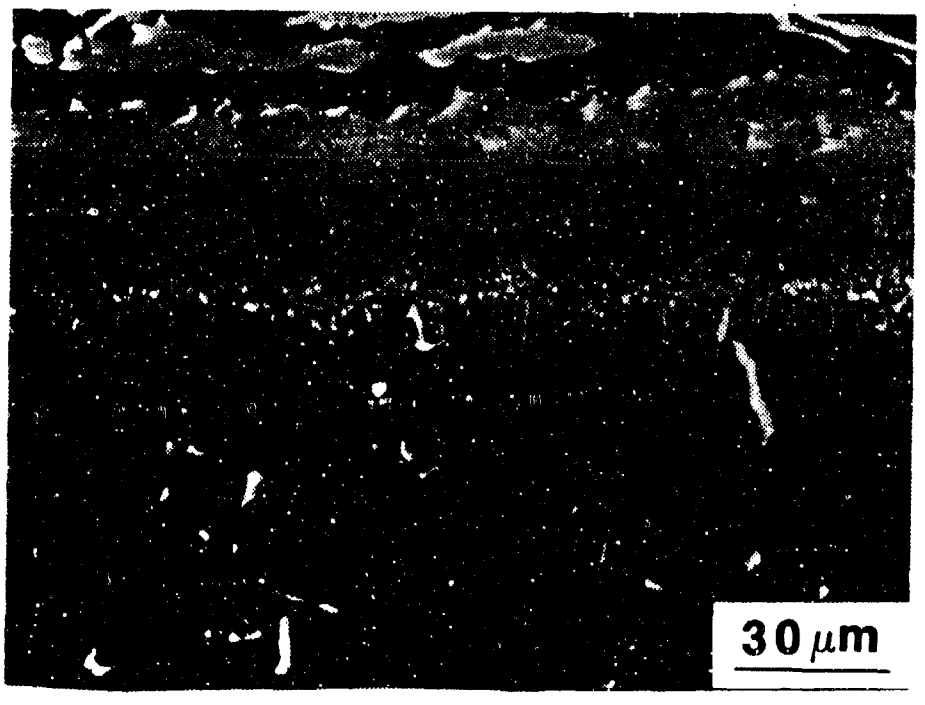

Figure B.13(b) LTHA Platinum-Aluminide/IN-738 (HTHC-200 hrs). Pre-Aluminizing Diffusion Heat Treatment (1925°F/1 hr)

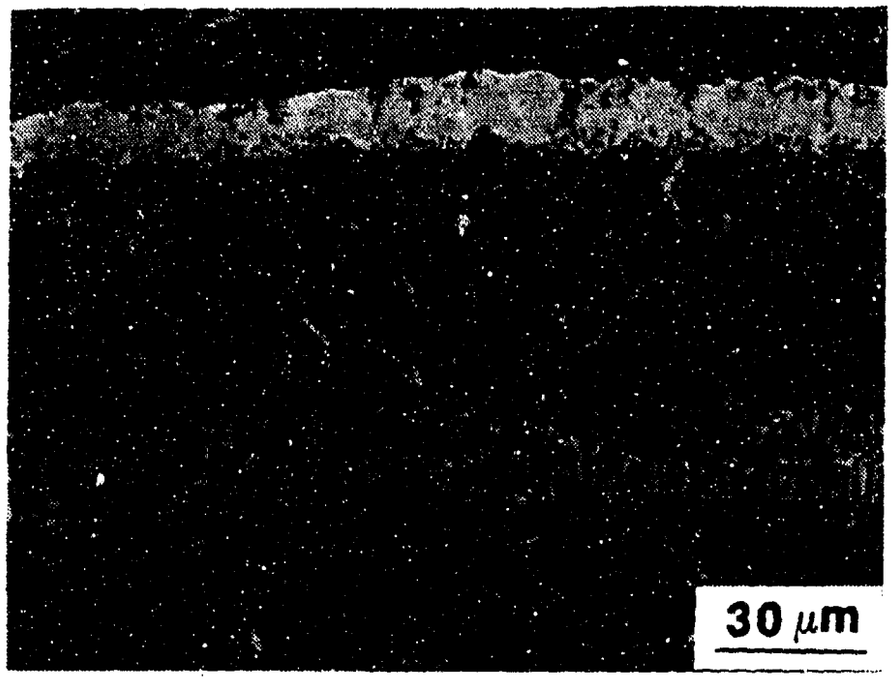

Figure B.14(a) LTHA Platinum-Aluminide/IN-738 (as-received). Pre-Aluminizing Diffusion Heat Treatment (1600°F/½ hr)

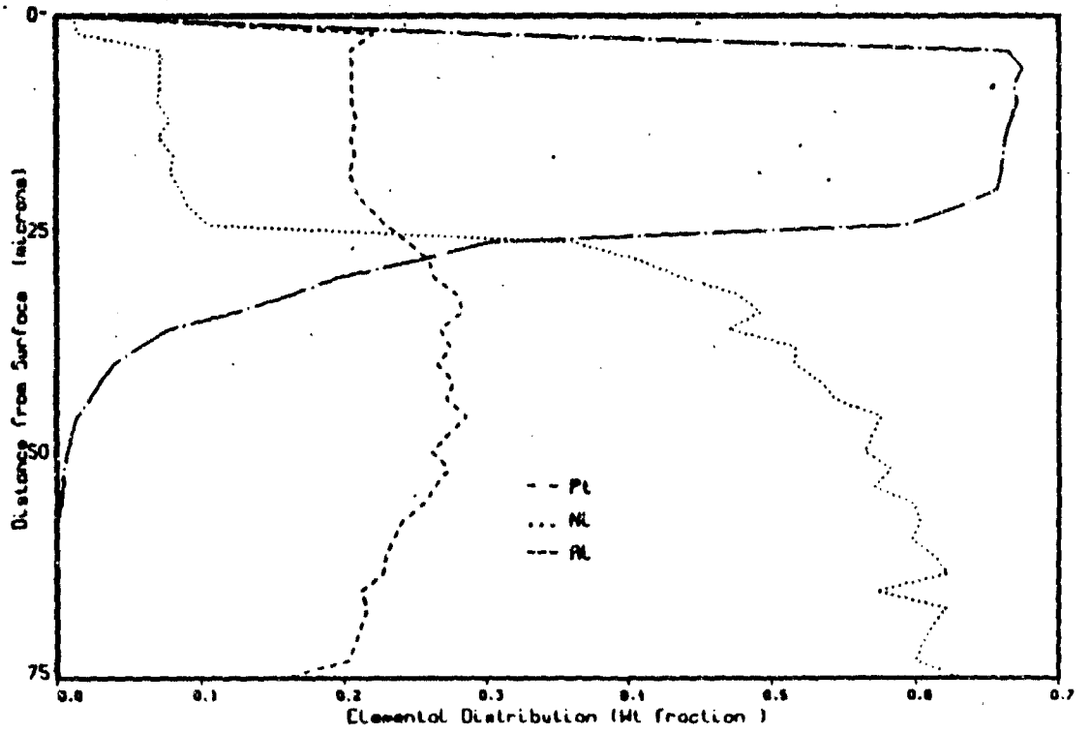

Figure B.14(b) Composition of LTHA Platinum - Aluminide/IN-738. Pre-Aluminizing Diffusion Heat Treatment (1600°F/½ hr)

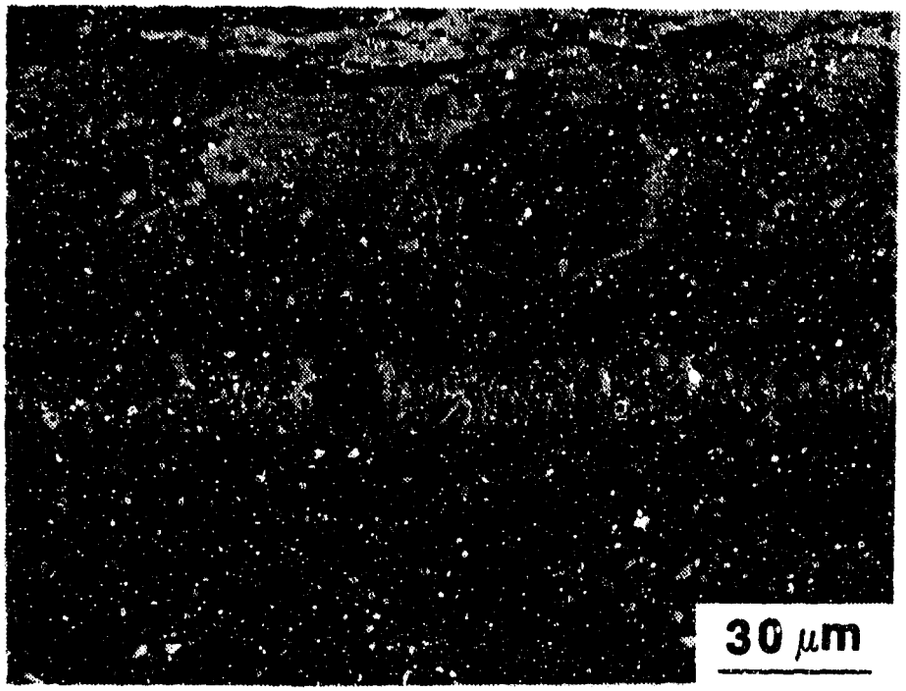

Figure B.15(a) LTHA Platinum - Aluminide/IN-738 (LTHC-100 hrs). Pre-Aluminizing Diffusion Heat Treatment (1600°F/½ hr)

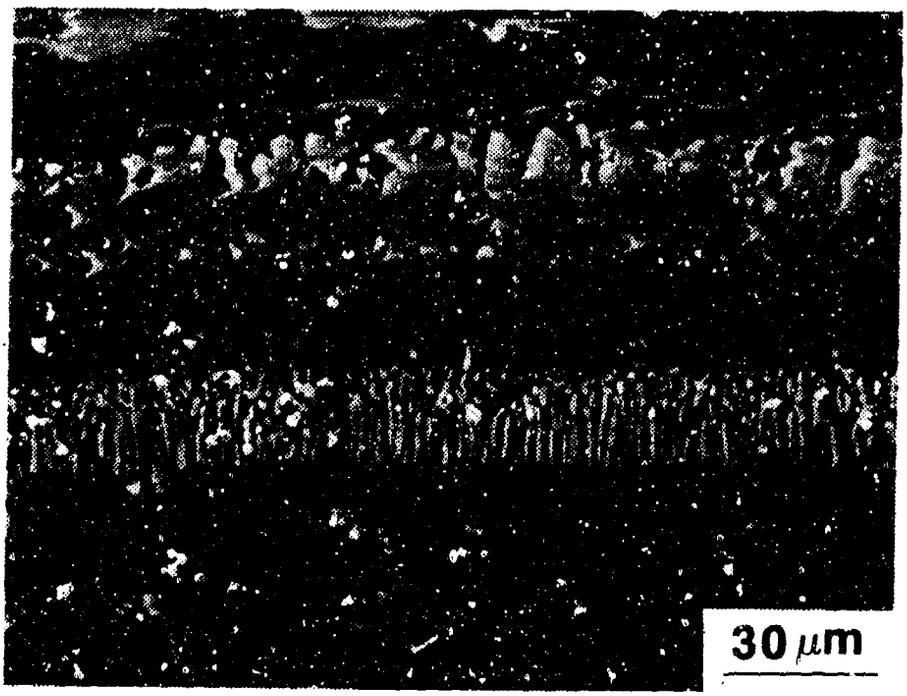

Figure B.15(b) LTHA Platinum-Aluminide/IN-738 (HTHC-200 hrs). Pre-Aluminizing Diffusion Heat Treatment (1600°F/½ hr)

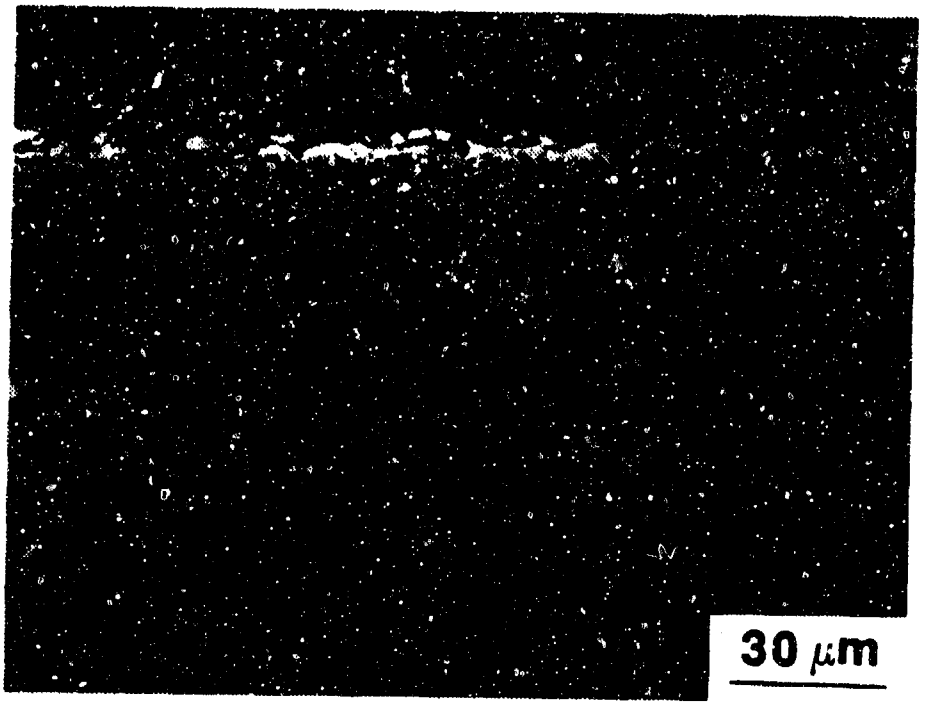

Figure B.16(a) ITIA Platinum-Aluminide/IN-738 (as-received).

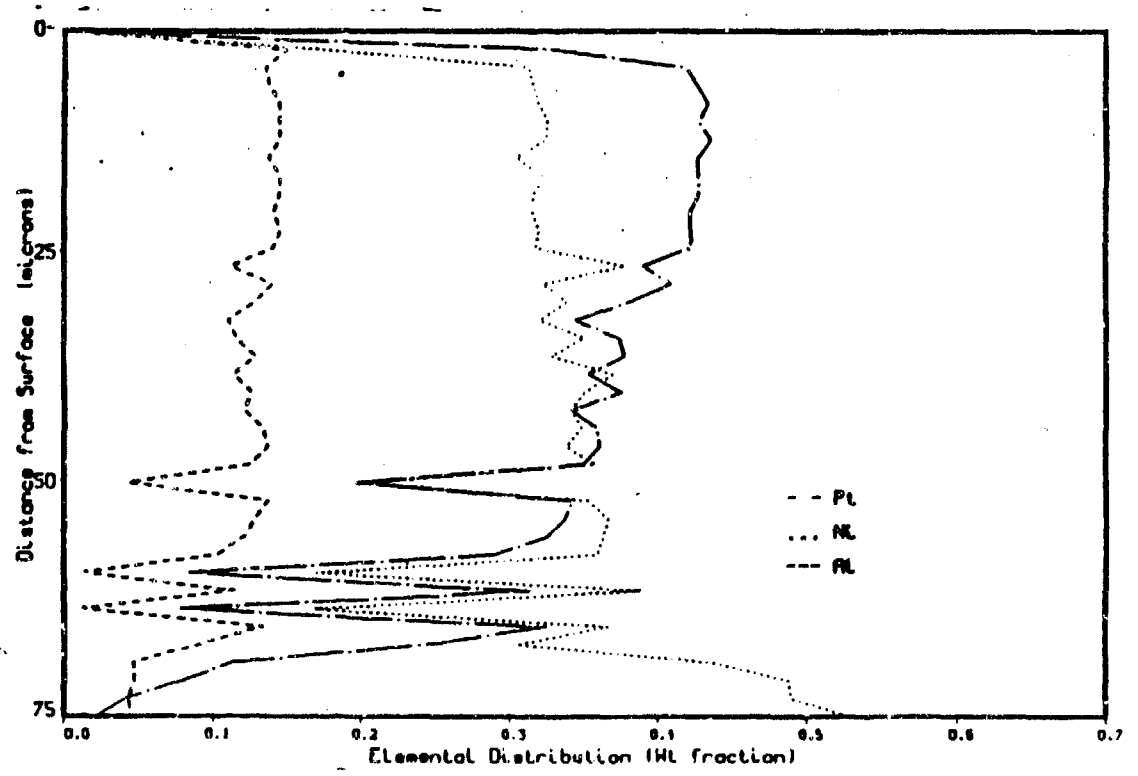

Figure B.16(b) Composition of ITIA Platinum-Aluminide/IN-738.

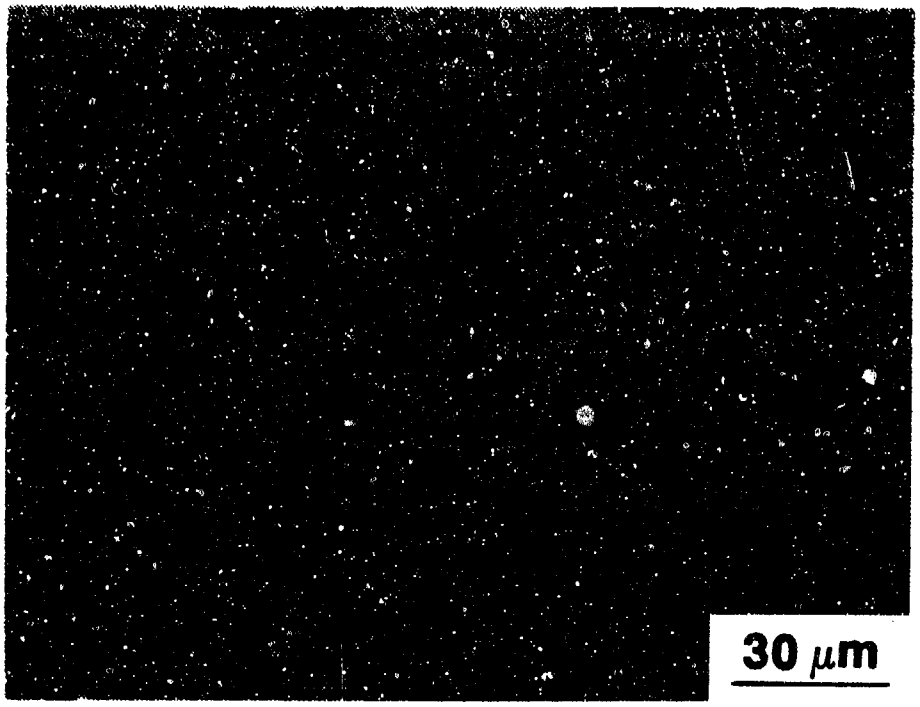

Figure B.17(a) ITIA Platinum-Aluminide/IN-738 (LTHC-100 hrs).

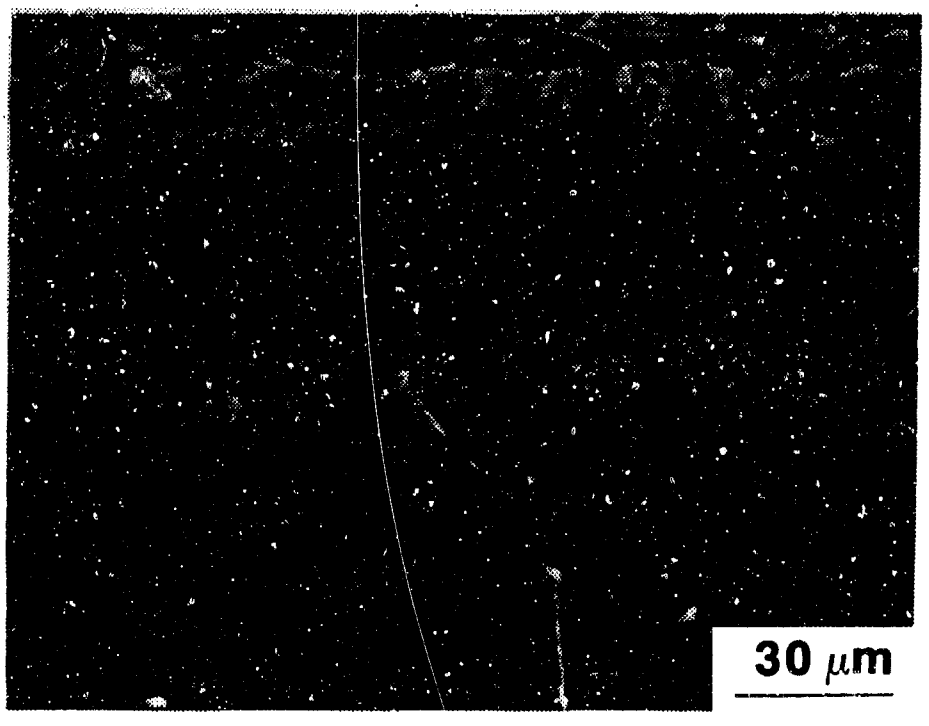

Figure B.17(b) ITIA Platinum-Aluminide/IN-738 (HTHC-200 hrs).

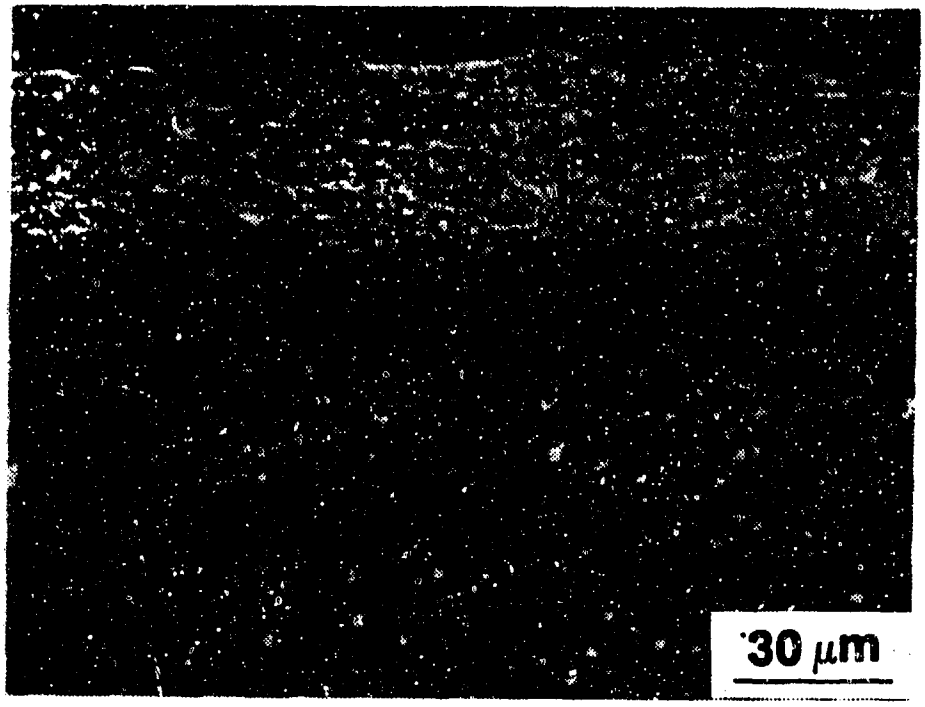

Figure B.18(a) HTLA Platinum-Aluminide/IN-738 (as-received).

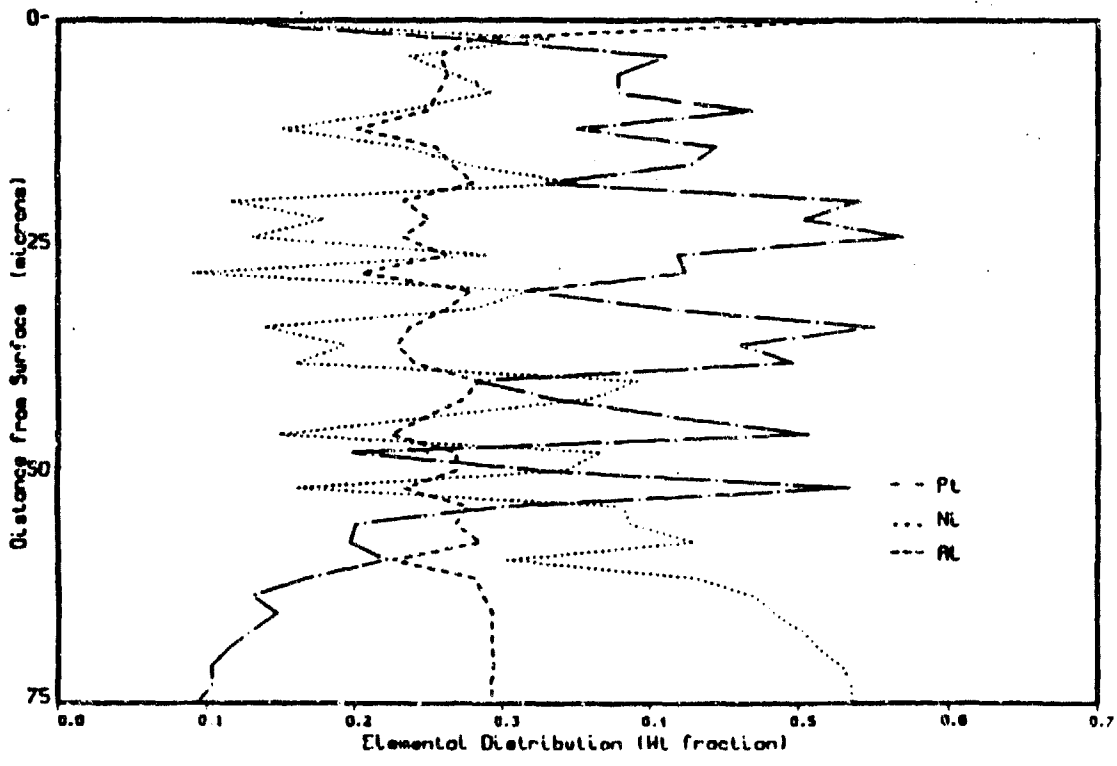

Figure B.18(b) Composition of HTLA Platinum-Aluminide/IN-738.

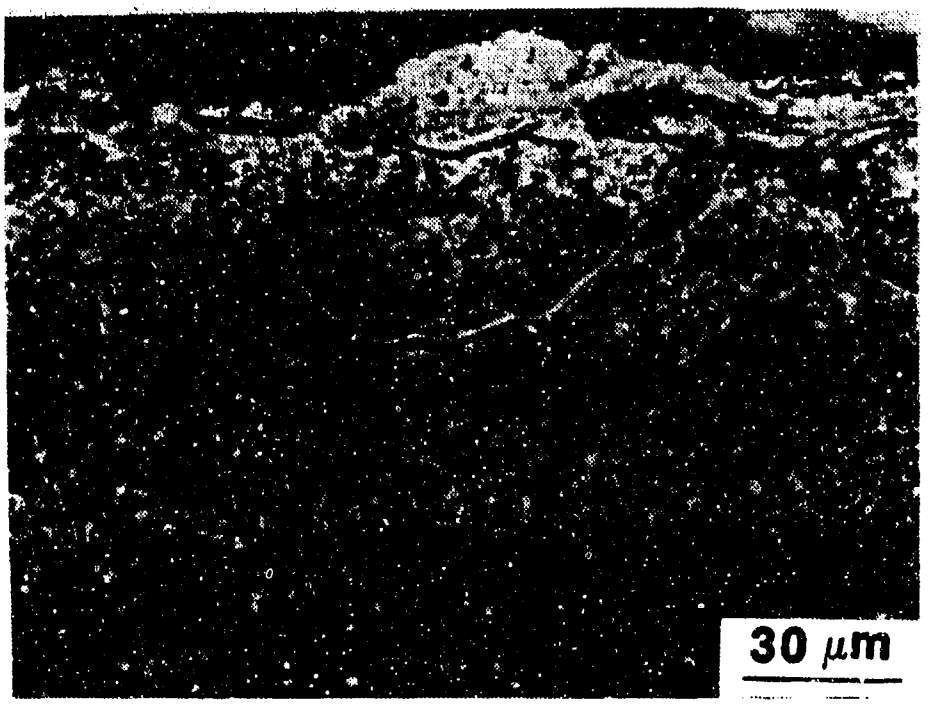

Figure B.19(a) HTLA Platinum-Aluminide/IN-738 (LTHC-100 hrs).

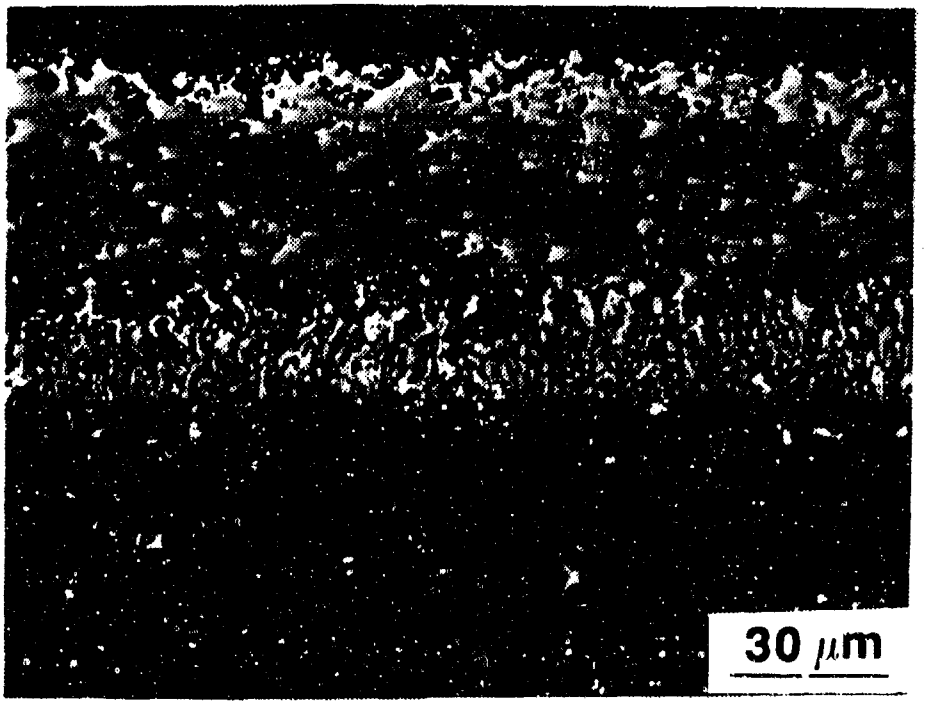

Figure B.19(b) HTLA Platinum-Aluminide/IN-738 (HTHC-200 hrs).

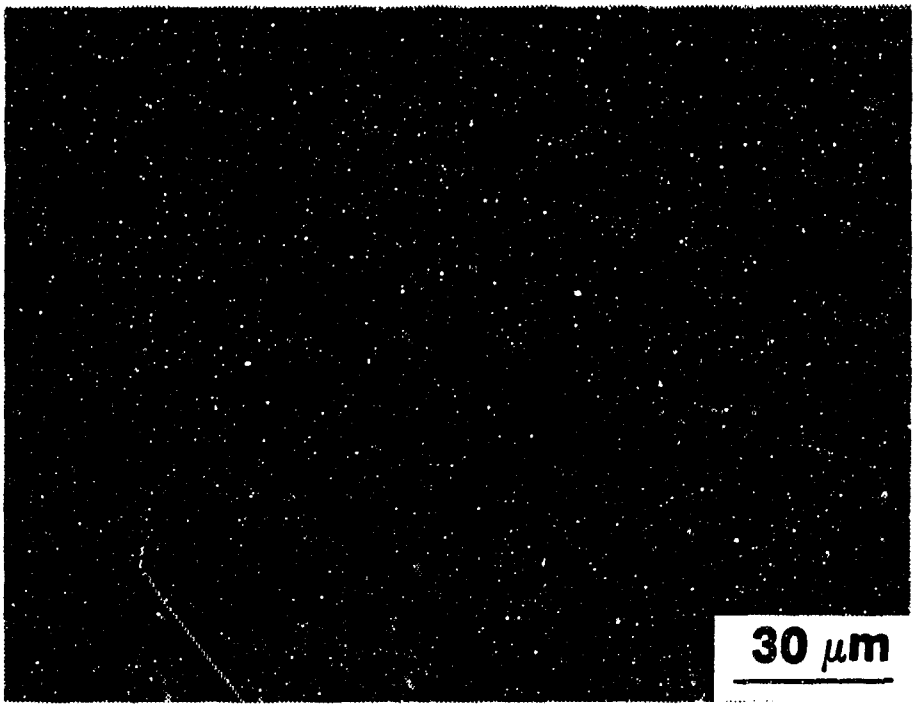

Figure B.20(a) Pt + (Cr + Al) - Single Step/IN-738 (as-received).

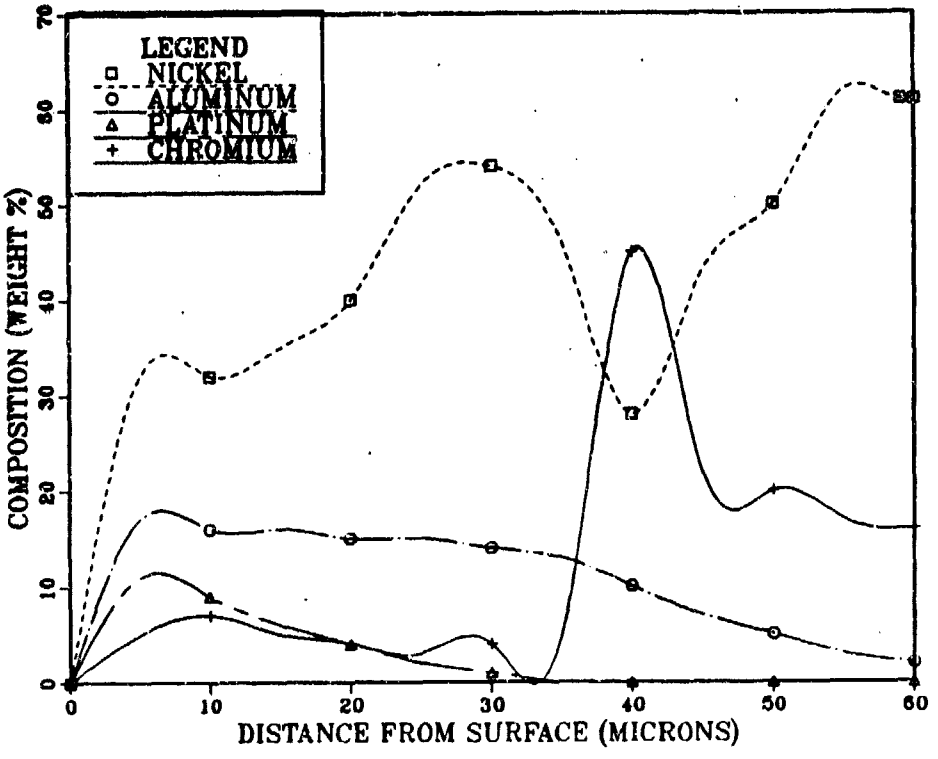

Figure B.20(b) Composition of Pt + (Cr + Al) - Single Step/ IN-738.

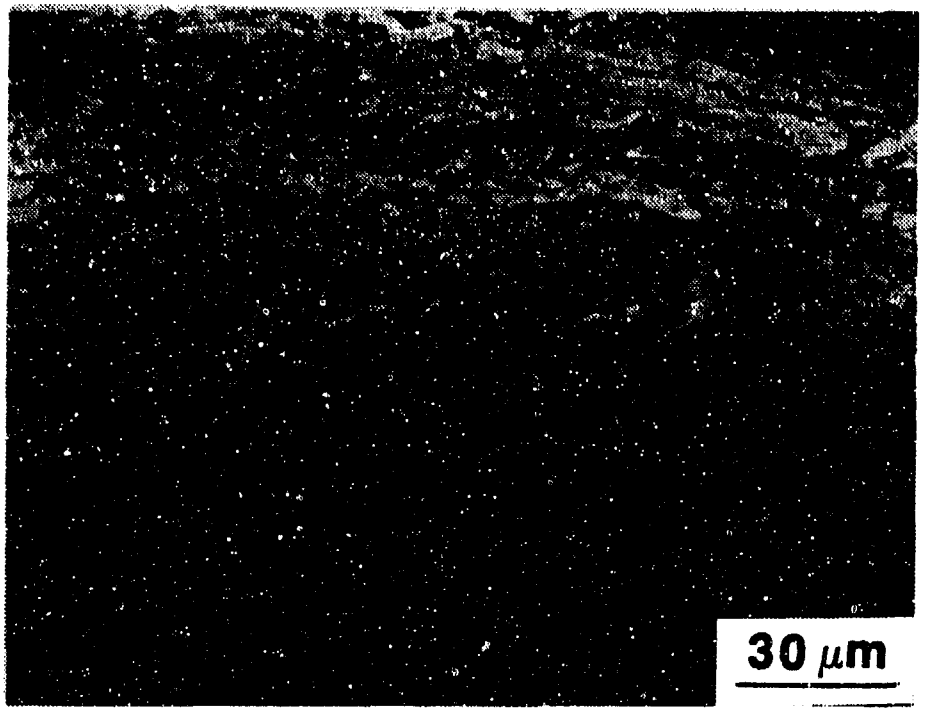

Figure B.21(a) Pt + (Cr + Al) - Single Step/In-738 (LTHC-100 hrs).

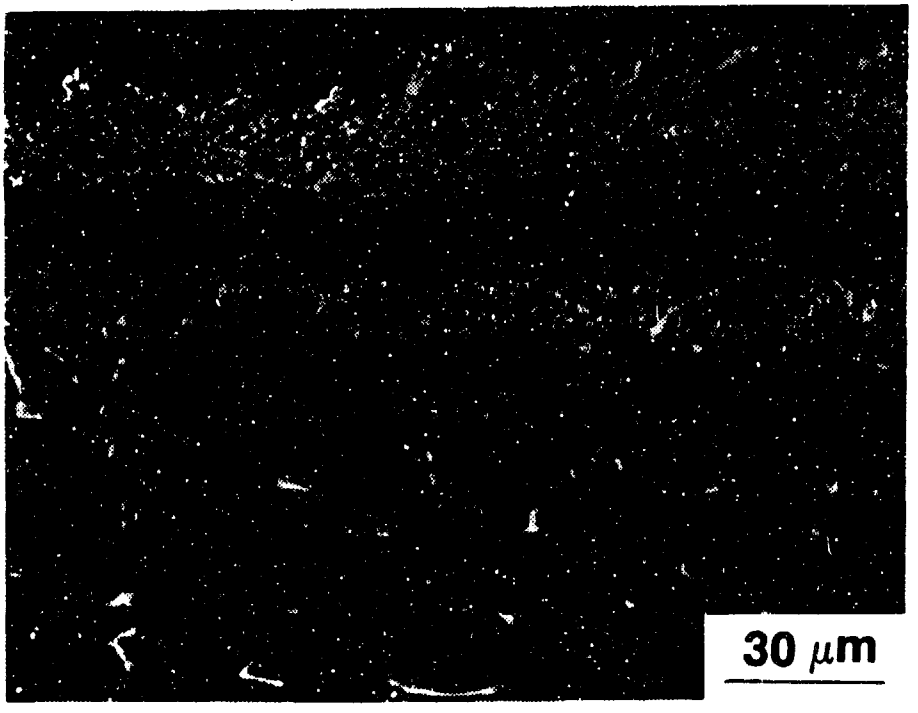

Figure B.21(b) Pt + (Cr + Al) - Single Step/ In-738 (HTHC-200 hrs).

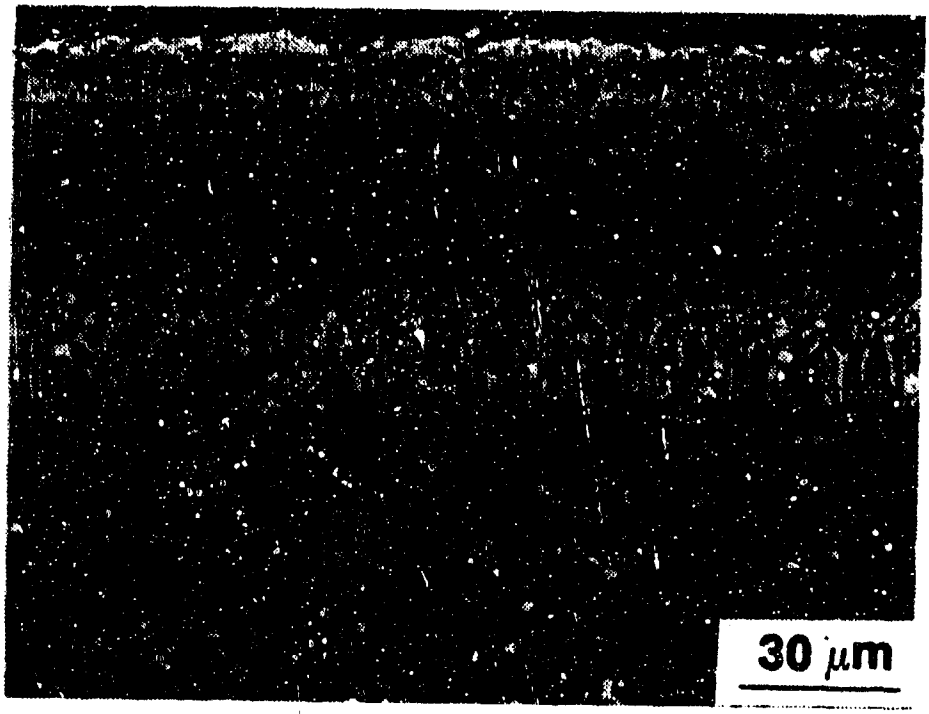

Figure B.22(a) Process B/In-738 (as-received).

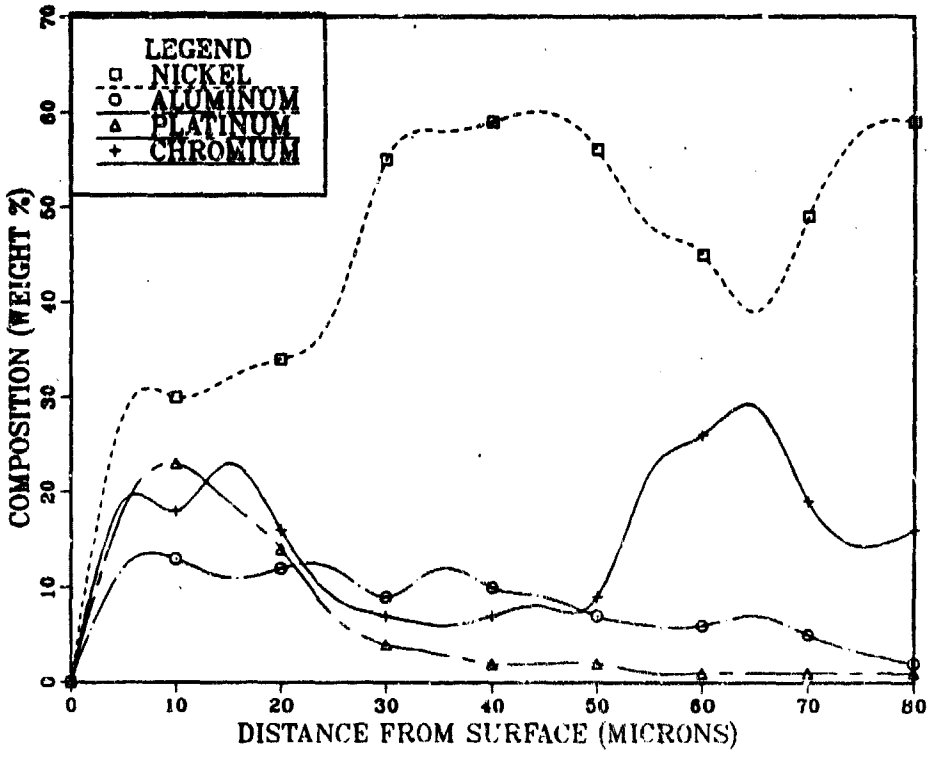

Figure B.22(b) Composition of Process B/In-738.

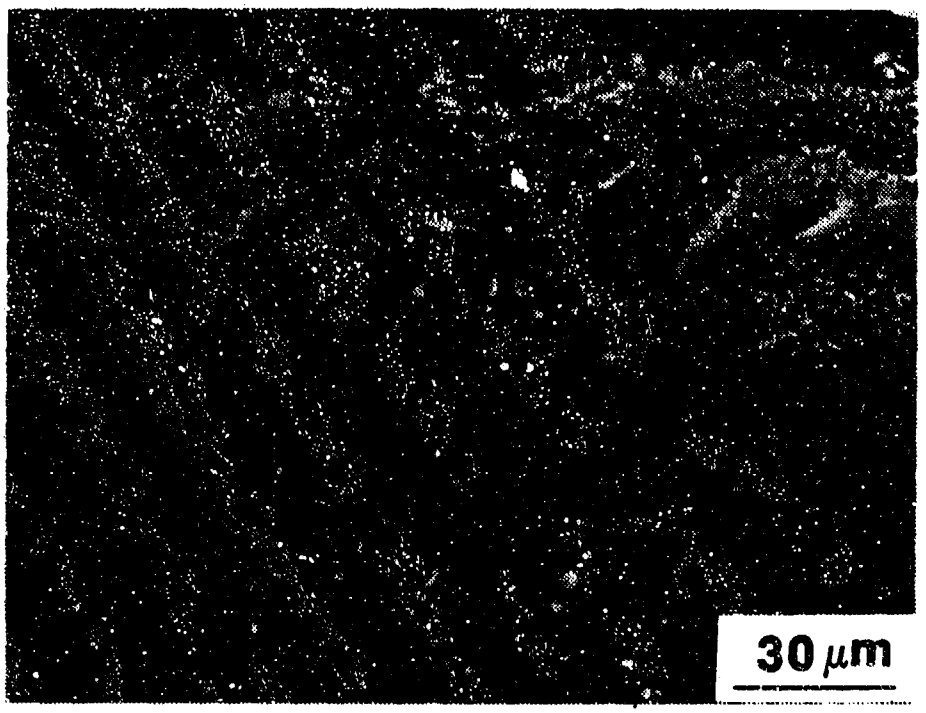

Figure B.23(a) Process B/IN-738 (LTHC-100 hrs).

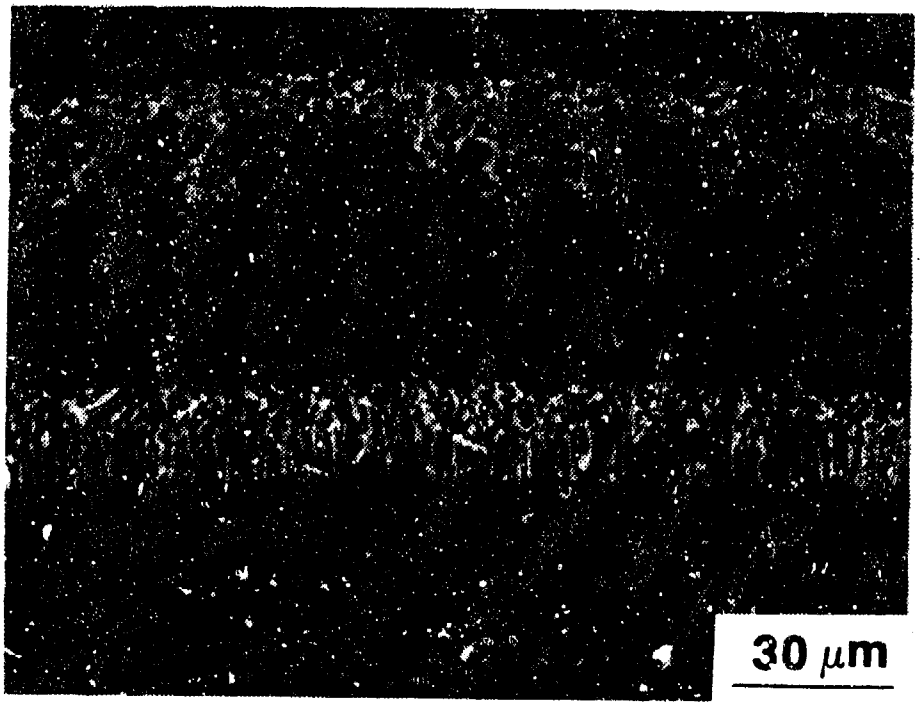

Figure B.23(b) Process B/IN-738 (HTHC-200 hrs).

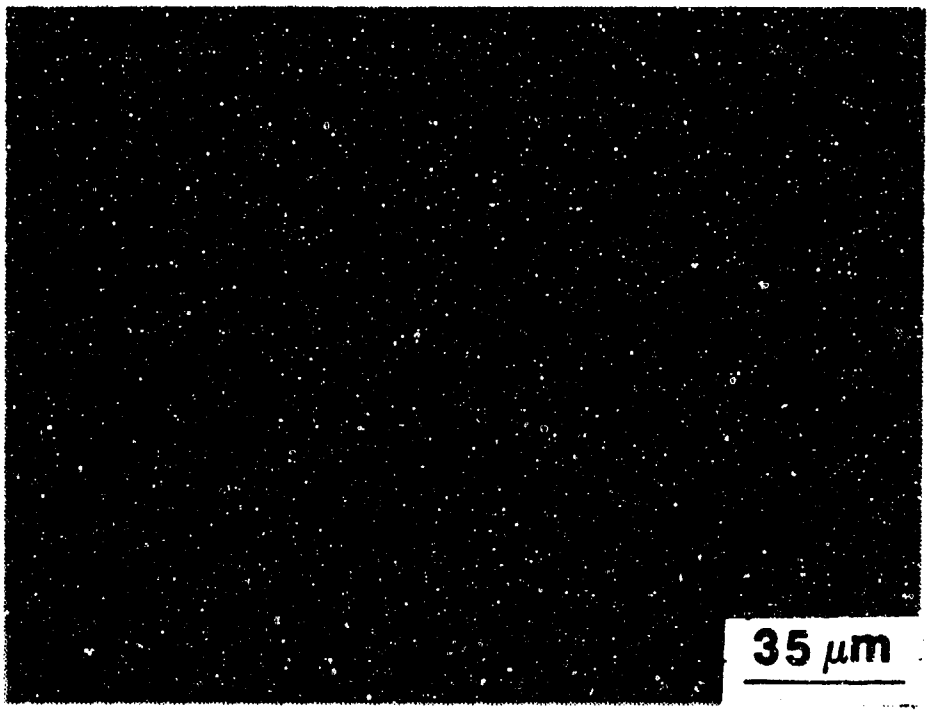

Figure B.24(a) Process D/IN-738 (as-received).

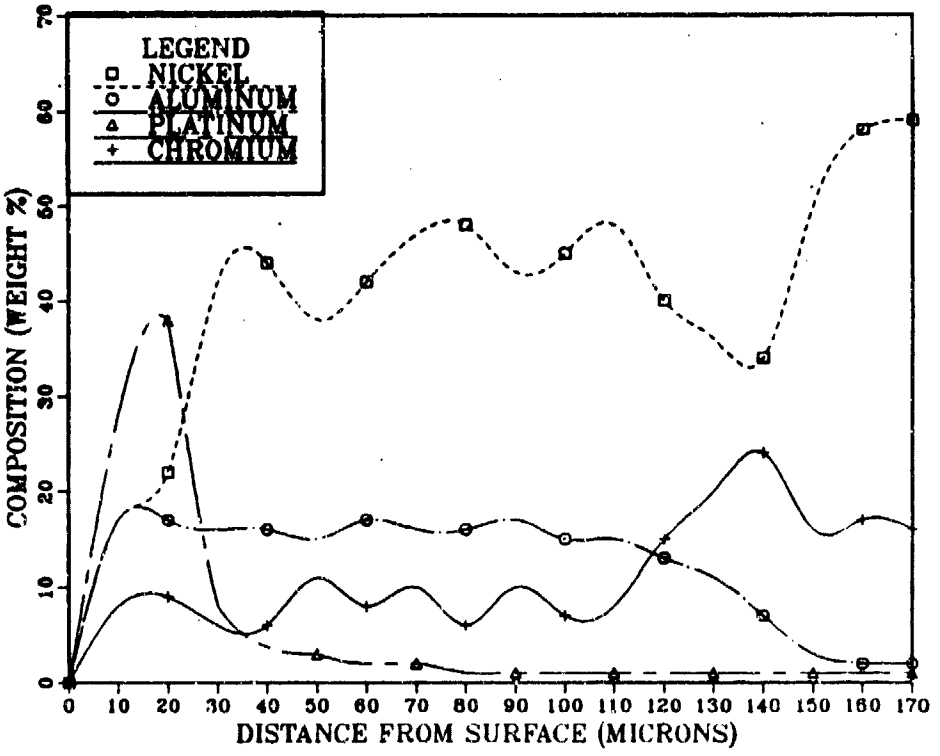

Figure B.24(b) Composition of Process D/IN-738.

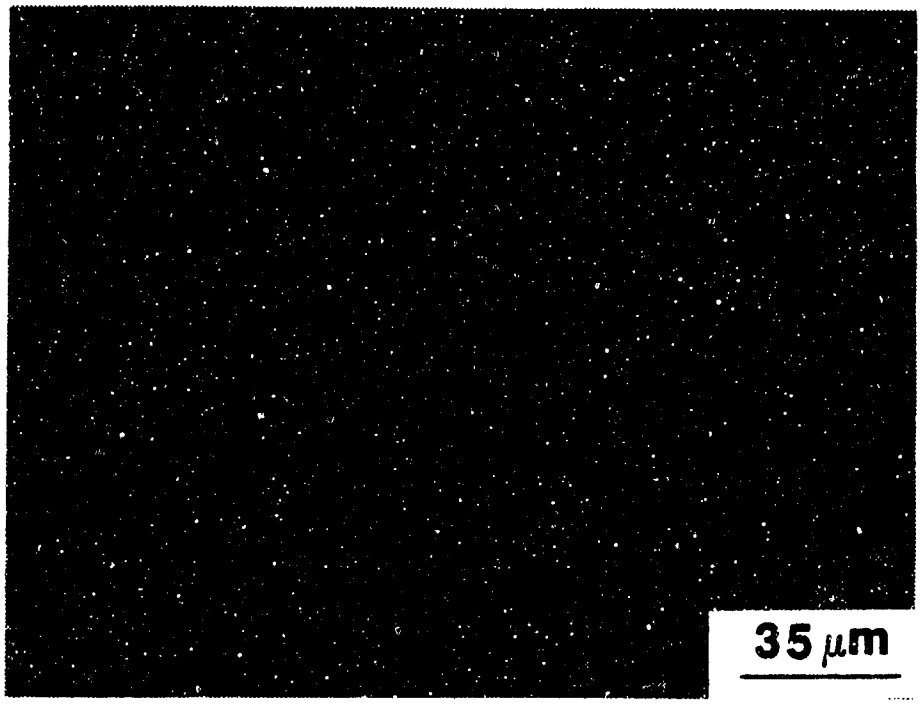

Figure B.25(a) Process D/IN-738 (LTHC-100 hrs).

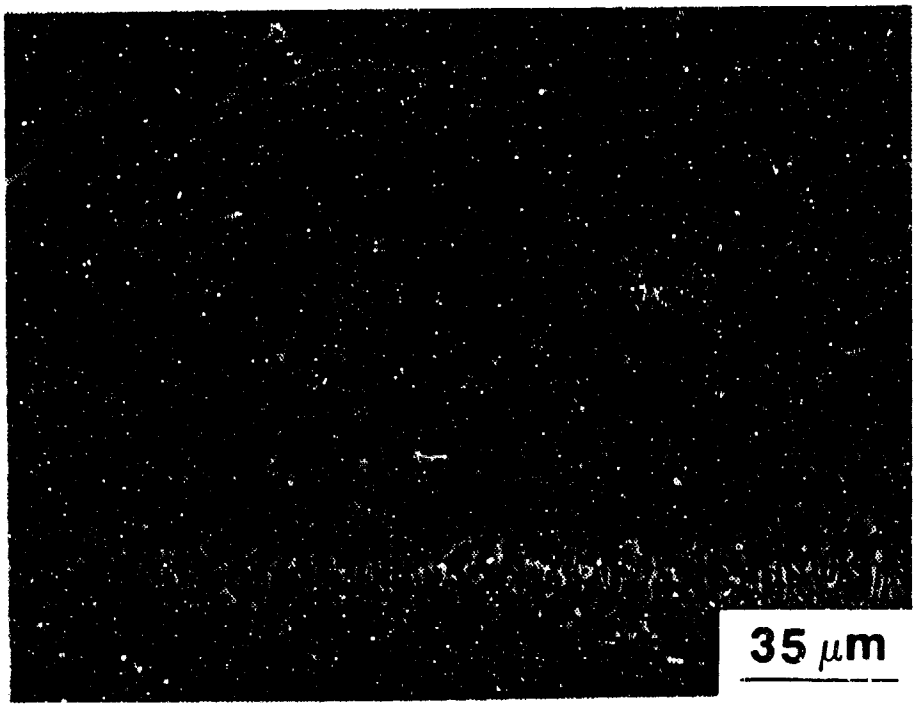

Figure B.25(b) Process D/IN-738 (HTHC-200 hrs).

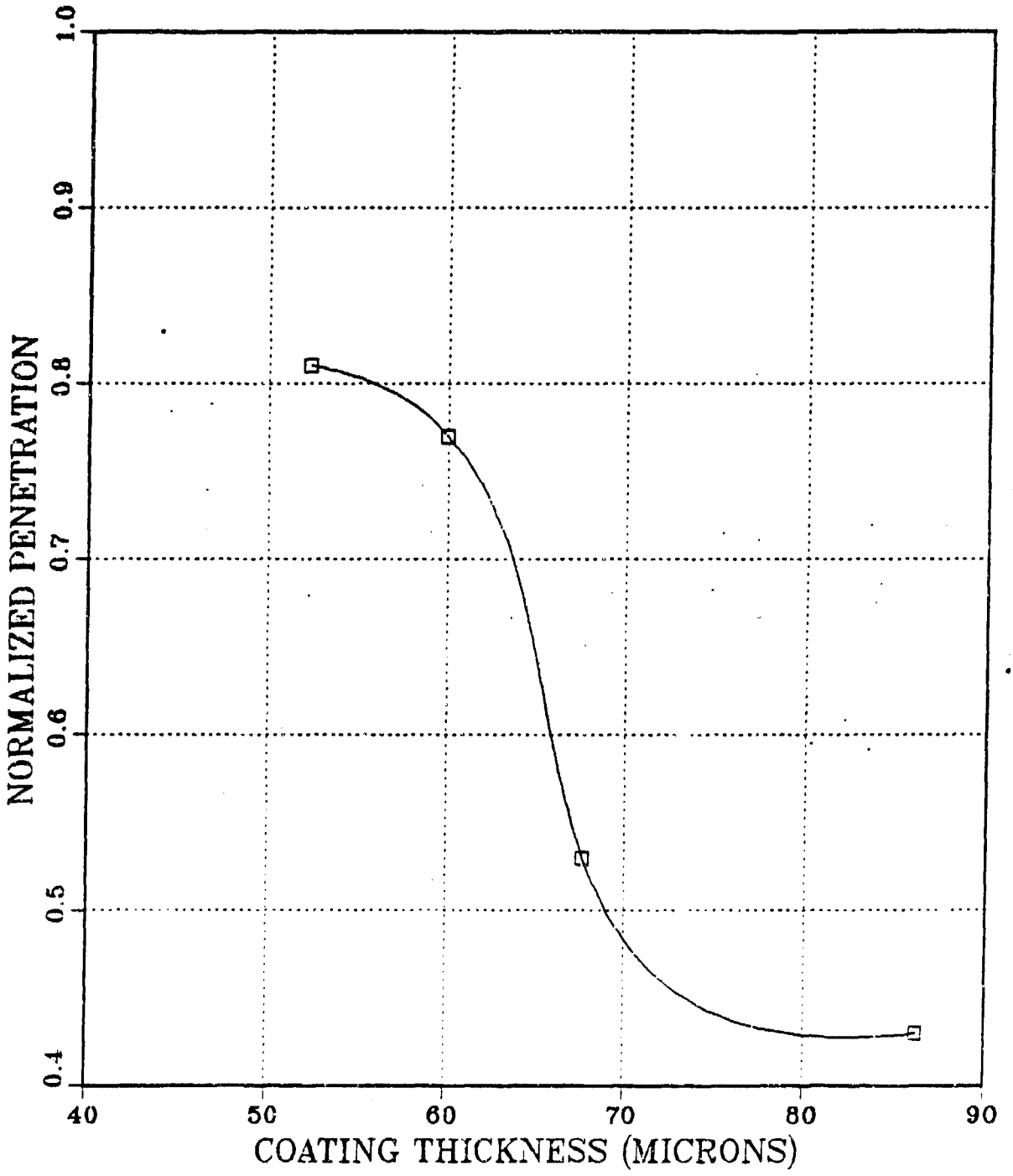

Figure B.26 Normalized Average Depth of Penetration (LTHC) vs Overall Coating Thickness.

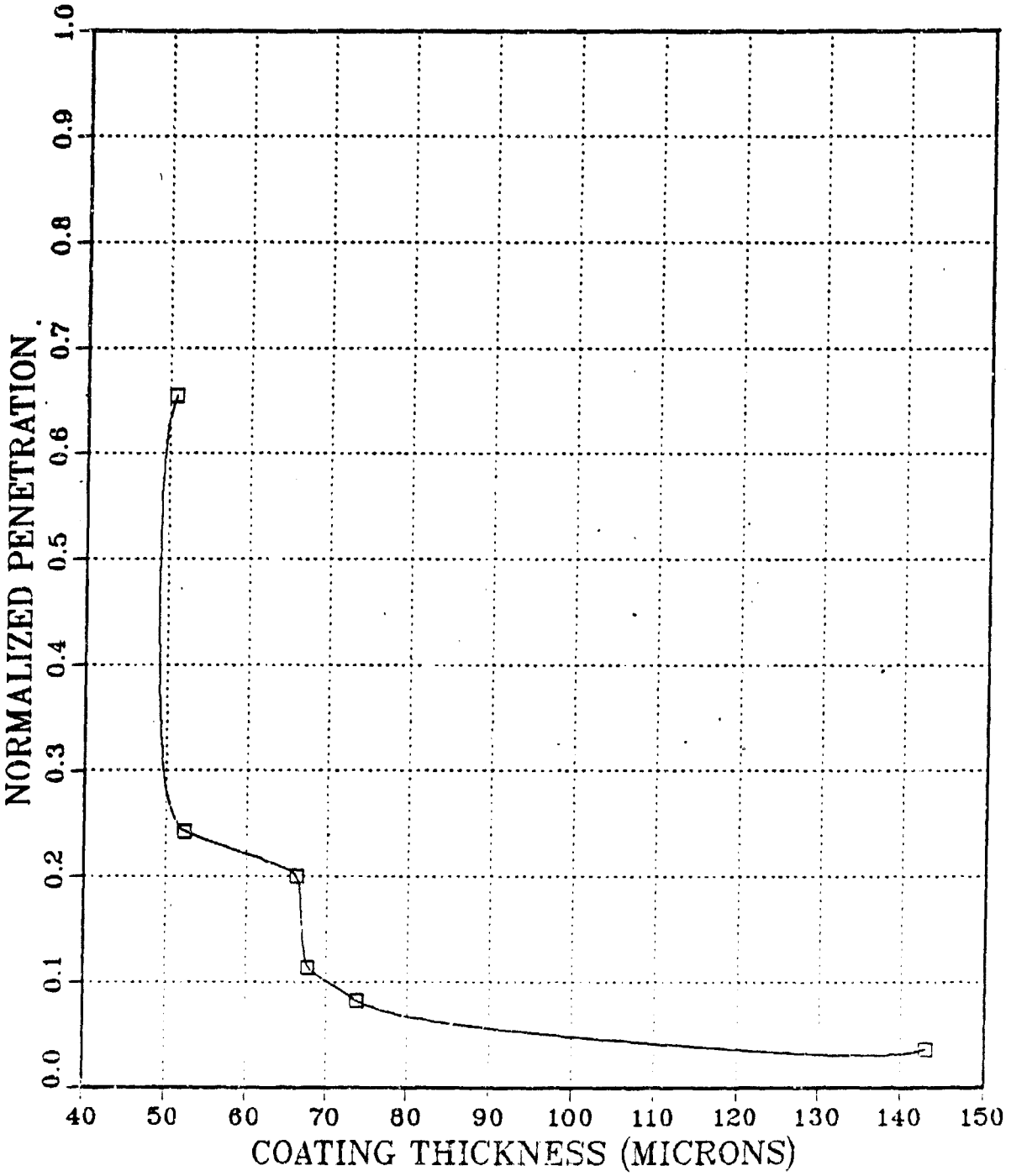

Figure B.27 Normalized Averaged Depth of Penetration (HTHC) vs Overall Coating Thickness.

LIST OF REFERENCES

1. Peterson, R. and Pyle, E., "Second Generation Gas Turbine," Naval Engineers Journal, pp. 38-42, August 1969.

2. Shepard, S.B., "NAVSEA Marine Gas Turbine Materials Development Program," Naval Engineers Journal, pp. 65-75, August 1981.

3. Zein, C., and others, "The Gas Turbine Ship Callaghan's First Two Years of Operation," Society of Naval Architects and Marine Engineers Transaction, v.77, pp. 344-371, November 1969.

4. Kear, B., "Advanced Metals," Scientific American, pp. 159-165, October 1986.

5. Donachie, M.J., Jr., "Introduction to Superalloys," Superalloys Source Book, American Society for Metals, 1984.

6. Naval Research Laboratory Memorandum Report 5070, Hot Corrosion in Gas Turbines, by R.L. Jones, 27 April 1983.

7. NASA Technical Memorandum 73878, High Temperature Environmental Effects on Metals, by S.J. Grisaffe and others, 22 August 1977.

8. Pettit, F.S. and Goward, G.W., "High Temperature Corrosion and Use of Coatings for Protection," Metallurgical Treatises, AIME Conference Proceedings, Beijing, China, pp. 601-605, 13-22 November 1981.

9. Pettit, F.S. and Meier, G.H., "Oxidation and Hot Corrosion of Superalloys," Superalloys 1984, AIME Conference Proceedings, Champion, Pennsylvania, pp. 653-656, 1984.

10. Pettit, F.S. and Goward, G.W., "Oxidation-Corrosion-Erosion Mechanisms of Environmental Degradation of High Temperature Materials," Coatings for High Temperature Applications, Applied Science Publishers, Ltd., 1983.

11. Pettit, F.S. and Meier, G.H., Superalloys 1984, Metallurgical Society of AIME, pp. 665-684, 1984.

12. American Society of Mechanical Engineers, paper 84-GT-277, A Long-Term Field Test of Advanced Gas Turbine Airfoil Coatings Under a Severe Industrial Environment, by K.G. Kubarych, D.H. Boone, and R.L. Duncan, pp. 1-2, 1983.

13. Pettit, F.S. and Goward, G.S., "High Temperature Corrosion and use of Coatings for Protection," Metallurgical Treatises, pp. 603-619, 1981.

14. Villat, M. and Felix, P., "High-Temperature Corrosion Protective Coatings for Gas Turbines," Sulzer Technical Review, Vol. 3, pp. 97-104, 1977.

15. Goward, G.W., Protective Coatings for High Temperature Gas Turbine Alloys, paper presented at the NATO Advanced Study Institute for Surface Engineering, Les Arcs France, 30-15 July 1983.

16. Seelig, R.P. and Steuber, R.J., "High Temperature Resistant Coatings for Superalloys," High Temperatures High Pressures, Vol. 10, pp. 209-213, 1978.

17. Goward, G.W. and Boone D.H., "Mechanisms of Formation of Diffusion Aluminide Coatings on Nickel-base Superalloys", Oxidation of Metals, Vol. 3, pp. 475-477, 1971.

18. Boone D.H., Protective Coatings and Thin Processing, CEI High Performance Materials Lecture, Arlington, Virginia, 4-8 November 1985.

19. Lehnert, G. and Meinhardt, H.W., "A New Protective Coating for Nickel Alloys," Electrodeposition and Surface Treatment, Vol. 1, pp. 189-193, 1972.

20. Streiff, R. and Boone, D.H., "The Modified Aluminide Coatings - Formation Mechanisms of Cr and Pt Modified Coatings," Reactivity of Solids, Elsevier Science Publisher, B.V., pp. 195-198, 1985.

21. Dust, M., and others, "Hot Corrosion Resistance of Chromium Modified Platinum-Aluminide Coatings," paper presented at the Gas Turbine Conference, Dusseldorf, West Germany, June 1986.

22. Wing, R.G. and McGill, I.R., "The Protection of Gas Turbine Blades -- A Platinum Aluminide Diffusion Coating," Platinum Metals Revue, Vol. 24, No. 3, p. 94, 1981.

23. Deb, P., Boone, D.H., and Streiff, R., "Platinum Aluminide Coating Structural Effects on Hot Corrosion Resistance at 900°C," Paper presented for publication in Journal of Vacuum Science and Technology, December 1985.

24. American Society of Mechanical Engineers, paper 85-GT-60, Low-Temperature Hot Corrosion in Gas Turbines: A Review of Causes and Coatings Therefor, by G.W. Goward, p.3, 1985

25. Dust, M.W. The Effect of Chromium Addition to the Low Temperature Hot Corrosion Resistance of Platinum Modified Aluminide Coatings. Master's Thesis, Naval Postgraduate School, Monterey, California, December 1985.

26. Strieff, R. and Boone, D.H., "Structure of Platinum Modified Aluminide Coatings," paper presented at the NATO Advanced Study Institute on Surface Engineering, Les Arcs, France, 3 July 1983.

27. Goebel, J.A., Barkalow, R.H., and Pettit, F.S., "The Effects Produced by Platinum in High Temperature Metallic Coatings," Proceedings of the Tri-Service Conference on Corrosion, MCIC Report No. 79-40, pp. 165-185, 1979.

28. Deb, P., Boone, D.H., and Streiff, R., "Effects of Microstructural Morphology on the Performance of Platinum Aluminide Coatings." Paper to be published in the Proceedings of the ASM Symposium--Coatings for High Temperature Oxidation Resistance, Toronto, Canada, October 1985.

29. Sims, C.T. and Hagel, W.C., eds., The Superalloys, John Wiley and Sons, Inc., pp. 318-322, 1972.

30. American Society for Metals, Metals Handbook, Desk Edition, 1985.

BIBLIOGRAPHY

Aprigliano, L.F., David W. Taylor Naval Ship Research and Development Center Report TM 28-78/218, Low Temperature (1300°F) Burner Rig Test of MCrAlY Composition Variations, September 26, 1978.

Boone, D.H., and Goward, G.W., The Use of Nickel-Aluminum Intermetallic Systems as Coatings for High Temperature Nickel Base Alloys, paper presented at the 3rd Bolton Landing Conference on Ordered Alloys Structural Application and Physical Metallurgy, September 1969 and published in the proceedings, 1970.

Cocking, J.L., Johnston, G.J., and Richards, P.G., "Protecting Gas Turbine Components," Platinum Metals Review, Vol. 29, No. 1, 1985.

Cooper,S.P. and Strang, A., "High Temperature Stability of Pack Aluminide Coatings on IN-738LC," High Temperature Alloys for Gas Turbines 1982, D. Reidel Publishing Company, 1982.

Felten, E.J. and Pettit, F.S., "Development, Growth, and Adhesion of Al_2O_3 on Platinum-Aluminum Alloys," Oxidation of Metals, Vol. 10, 1976.

Goward, G.W. and Boone, D.H., "Mechanisms of Formation of Diffusion Aluminide Coatings on Nickel-Base Superalloys," Oxidation of Metals, Vol. 3, No. 5, 1971.

Goward, G.W., Protective Coatings - Purpose, Role, and Design, paper presented at the Royal Society Coating Symposium, London, England, November 1984.

Hanna, M.D., "The Formation of Platinum Aluminide Coatings on IN 738 and Their Oxidation Resistance," Ph.D. Thesis, Sheffield University, Sheffield, England, 1982.

Jackson, M.R. and Rairden, J.R., "The Aluminization of Platinum and Platinum-Coated IN-738," Metallurgical Transactions, Vol. 8A, November 1977.

Johnson, G.R. and Richards, P.G., "Relative Durabilities of Conventional and Platinum-Modified Aluminide Coatings in an Operational Gas-Turbine Engine," Proceedings of the Symposium on Corrosion in Fossil Fuel Systems, ECS Fall Meeting, Detroit, Michigan, 17-21 October 1982.

Jones, R.L., Stern, K.H., Deanharde, M.L., and Halle, J.C., "Hot Corrosion Studies at the Naval Research Laboratory," Proceedings of the 4th Conference on Gas Turbine Materials in a Marine Environment, Annapolis, Maryland, June 1979.

Malik, M., Morbioli, R. and Huber, P., "The Corrosion Resistance of Protective Coatings," High Temperature Alloys for Gas Turbines 1982, D. Reidel Publishing Company, 1982.

Pettit, F.S., "Design of Structural Alloys with High Temperature Corrosion Resistance," in Fundamental Aspects of Structural Alloy Design, R.I. Jaffee and B.A. Wilcox, Plenum Press, New York, 1976.

Pichior, R., "Influence of the Mode of Formation on the Oxidation and Corrosion Behavior of NiAl-Type Protective Coatings," Materials and Coatings to Resist High Temperature Corrosions, Applied Science Publishers, London, 1978.

Restall, J.E., "High Temperature Coatings for Protecting Hot Components in Gas Turbine Engines," Metallurgia, November 1979.

Shankar, S. and Seigle, L.L., "Interdiffusion and Intrinsic Diffusion in the NiAl(delta) Phase of the Al-Ni System," Metallurgical Transactions, Vol. 9A, October 1978.

Sims, C.T., A History of Superalloy Metallurgy for Superalloy Metallurgists, CEI High Performance Materials Lecture, Arlington, Virginia, 4-8 November 1985.

Steinmetz, P., and others, "Hot Corrosion of Aluminide Coatings on Nickel-Base Superalloys," High Temperature Protective Coatings, The Metallurgical Society of AIME, 1983.

Versnyder, F.L., "Superalloy Technology - Today and Tomorrow," High Temperature Alloys for Gas Turbines 1982, D. Reidel Publishing Company, 1982.

INITIAL DISTRIBUTION LIST

	No. Copies
1. Defense Technical Information Center Cameron Station Alexandria, Virginia 22304-6145	2
2. Library, Code 0142 Naval Postgraduate School Monterey, California 93943-5002	2
3. Department Chairman, Code 69 Department of Mechanical Engineering Naval Postgraduate School Monterey, California 93943-5000	1
4. Adjunct Professor D.H. Boone, Code 69Bl Department of Mechanical Engineering Naval Postgraduate School Monterey, California 93943-5000	4
5. Professor T.R. McNelley, Code 69Mc Department of Mechanical Engineering Naval Postgraduate School Monterey, California 93943-5000	3
6. Commander, Naval Air Systems Command Department of the Navy (803) Washington, D.C. 20361	1
7. Lt. Rudolph E. Malush, USN 45 Central Avenue Charleroi, Pennsylvania 15022	4